University of Lisbon

Faculty of Pharmacy

Multicomponent nanoplatform as a vaccine against brain tumors

Madalena de Ayala Botto Ferreira Alves

Dissertation supervised by Professor Doutor Helena Florindo and co-supervised by Dr João Conniot

Master in Biopharmaceutical Sciences

2020

University of Lisbon

Faculty of Pharmacy

Multicomponent nanoplatform as a vaccine against brain tumors

Madalena de Ayala Botto Ferreira Alves

Dissertation supervised by Professor Doutor Helena Florindo and co-supervised by Dr João Conniot

Master in Biopharmaceutical Sciences

2020

Abstract

Vaccination is a promising strategy to trigger and boost immune responses against cancer. Biodegradable polymeric nanoparticles (NPs) are promising vaccine delivery systems due to their capacity to entrap antigens and immunoadjuvants, allowing for their sustained release over time, protection from *in vivo* degradation, while ensuring specific targeting of antigen-presenting cells (APCs).

We have synthesized and characterized aliphatic-polyester (poly(lactic-co-glycolic acid) (PLGA) NPs co-entrapping CpG oligodeoxynucleotides (CpG) and polyinosinic:polycytidylic acid (Poly (I:C)) adjuvants with neo-antigens expressed in melanoma and glioblastoma tumor cells to investigate the impact of nanoparticles' properties in the activation and subsequent maturation of APCs, namely dendritic cells (DCs), aiming at the generation of antigen-specific immune responses in primary and metastatic brain tumors. Several types of NPs were produced – non-targeted poly(lactic acid)/poly(lactic-co-glycolic acid)-pol(ethylene glycol) (PLA/PLGA-PEG), PLA/PLGA and PLGA-PEG NP, or targeted PLA/PLGA-PEG-Mannose and PLA/PLGA-Mannose NPs, to improve NP targeting and internalization by APCs.

All NPs had physicochemical properties adequate for DC targeting, with an average size below 200 nm and narrow particle size distribution. PLA/PLGA-PEG and PLA/PLGA-PEG-Mannose NPs presented lower mean diameters and higher DC internalization values than those obtained for PLGA-PEG NPs. Independently of NP composition, all PLGA-PEG, PLA/PLGA-PEG and PLA/PLGA-PEG-Mannose NPs revealed to be non-toxic to immature DCs line, with cell viability higher than 80%.

Due to the advantages of PLA-based NPs and the role that PF-127 may have, it was investigated the impact of different polymers (PLA/PLGA, PLA/PLGA-Mannose and PLA/PLGA-PEG-Mannose) and surfactants (PVA and PF-127), on DC internalization and maturation.

All NPs efficiently entrapped glioblastoma and metastatic melanoma neo-antigens with CpG and Poly (I:C) and were preferentially internalized by migratory DCs. NPs containing the combination of neo-antigen expressed in glioblastoma or melanoma with adjuvants, successfully induced the maturation of migratory DCs, with increased expression of costimulatory and MHC molecules that are essential for antigen presentation and activation of naive T cells

Keywords: Adjuvants, Antigen presenting cells (APCs), Brain tumors, Cancer vaccines, Neo-antigens.

Resumo

Os tumores situados no sistema nervoso central (CNS) são a principal causa de morte de cancro entre crianças e adolescentes, sendo o glioblastoma multiforme o mais comum, com uma taxa de sobrevivência de apenas 5% após o seu diagnóstico. Além disso, as células tumorais de outros tumores primários, como por exemplo células de melanoma, conseguem ainda escapar e metastizar para outros órgãos, incluindo o cérebro. Uma vez o tumor presente no cérebro, o prognóstico associado é baixo, com uma esperança de vida até 14 meses.

O tratamento tradicional baseia-se na cirurgia mas, devido à localização destes tumores, a sua completa remoção é muito difícil e a radioterapia e a quimioterapia tendem a provocar tolerância e recorrência de células tumorais. Assim sendo, há uma grande urgência em desenvolver terapias mais eficazes e específicas para tumores cerebrais.

A iniciação e a progressão do cancro reflete um conjunto de mutações no mecanismo de reparo do DNA e ainda de alterações epigenéticas. Pensa-se que seja o conjunto destes dois tipos de anomalias que permita às células tumorais crescerem, sem que o sistema imunitário consiga impedi-las.

Devido às alterações genéticas, as células tumorais apresentam uma elevada taxa de proliferação. Quando a quantidade de oxigénio e nutrientes é insuficiente para assegurar o seu crescimento, as células tumorais libertam fatores induzidos por hipóxia (HIFs) que induzem uma angiogénese patológica. Durante este processo, a migração das células imunitárias diminui, enquanto que as células imunossupressoras se acumulam no microambiente tumoral. Além disso, as células tumorais também conseguem regular os mecanismos de resistência à apoptose e ainda inibir a atividade das células T que foram previamente ativadas. Todas estas estratégias utilizadas pelas células tumorais fazem com que haja um menor número de células imunitárias capazes de eliminar as células tumorais, assim como uma própria diminuição da atividade anti-tumoral destas. Como consequência, as células tumorais conseguem fugir ao controlo das células imunitárias, permitindo que continuem a proliferar e a metastizar para outros órgãos.

Uma terapia que tem vindo a ser utilizada é a imunoterapia activa, pois tem a capacidade de (re) ativar a capacidade do sistema imunológico do hospedeiro em reconhecer os antigénios associados a tumores (TAAs) e assim, desenvolver uma resposta específica e eficaz.

As células dendríticas (DCs) são consideradas células apresentadoras de antigénios (APC) profissionais capazes de estimular células T, as quais são fundamentais no desenvolvimento de uma resposta imune. As DCs imaturas localizadas nos tecidos periféricos

atuam como sentinelas. Elas sofrem maturação em resposta a diferentes estímulos que incluem componentes microbianos, tumorais e danos nos tecidos periféricos, promovendo a sua migração para os nódulos linfáticos (LN). Aqui, as DCs regulam a expressão de moléculas co-estimulatórias e dos complexos péptidos-moléculas do complexo de histocompatibilidade (MHC) de classe I e II, levando à estimulação das células T específicas para esse antigénio. Uma resposta citotóxica específica contra as células tumorais que expressam esse antigénio é depois induzida após a ativação destas células T e a sua subsequente diferenciação em linfócitos T citotóxicos (CTLs) e linfócitos T auxiliares (Th). A utilização de nanopartículas (NPs) é uma das estratégias utilizadas para prevenir a eliminação de antigénios e outras moléculas capazes de aumentar a resposta imunitária (adjuvantes).

No presente trabalho utilizaram-se NPs poliméricas biodegradáveis tendo em conta as seguintes vantagens: i) possível alteração da sua superfície para que se promova o transporte de moléculas ativadoras do sistema imunológico para as APCs, bem como a libertação controlada dos mesmos, reduzindo assim a sua frequência de administração; ii) aumentam a solubilidade das moléculas insolúveis em água; iii) são biocompatíveis uma vez que os produtos resultantes da sua degradação são o ácido lático e o glicólico, os quais são substrato do ciclo de Krebs, apresentando por isso baixa toxicidade. Estas NPs são portanto internalizadas por APC, sendo os péptidos libertados nos compartimentos intracelulares ou no citosol destas, permitindo o processamento e posterior apresentação dos antigénios por diferentes vias de sinalização, o que resultará numa extensa resposta imunológica.

O revestimento destas nanovacinas pelo polietilenoglicol (PEG) previne a eliminação destas do organismo antes que cheguem às APCs. Trata-se de um polímero hidrofilíco que reduz as interações entre as NPs e as biomoléculas presentes no sangue ou no líquido intersticial, o que faz com que o tempo de semi-vida destas aumente. Além disso, para assegurar que as NPs são fagocitadas especificamente pelas APCs, a superfície das NPs pode ser conjugada com ligandos de receptores presentes nessas células fagocitárias. Os receptores de lectina, por exemplo, aumentam o reconhecimento e internalização destas NPs, promovendo o processamento de antigénios. As NPs desenvolvidas neste trabalho foram funcionalizadas com manose, a qual se liga aos receptores CD206. Assim, com esta estratégia asseguramos que, além de as NPs serem específicas para as APCs, promoveremos a sua entrada mediada por receptores, pelo que se reforçará o possível processamento de antigénios por múltiplas vias, incluindo a sua libertação preferencial no citosol. Assim, estes epitopos serão apresentados após a sua conjugação com as moléculas MHC classe I (apresentação cruzada), o que levará à ativação das CTL.

Estas NPs foram preparadas com uma mistura de polímeros de poli(ácido láctico)/poli(ácido láctico-co-glicólico)-poli(etilenoglicol) (PLA/PLGA-PEG) (80:20), PLGA-PEG, PLA/PLGA (80:20) PLA/PLGA-PEG-Manose (80:20) e PLA/PLGA-Manose (80:20). Todas as partículas foram produzidas com poli(álcool vinílico) (PVA) na fase interna, vitamina E d-α-tocoferil polietilenoglicol 1000 succinato (TPGS) na fase externa e com PVA ou Pluronic (PF-127) na fase final, pelo método de dupla emulsão.

Primeiramente, o agente tensioativo ou estabilizador PVA previamente dissolvido na fase aquosa é misturado com o polímero dissolvido numa fase orgânica. Após a formação da primeira emulsão (o/w_1), um segundo agente tensioativo (TPGS) é misturado, originando uma segunda emulsão. A dupla emulsão resultante ($w_1/o/w_2$) é adicionada a uma fase aquosa de PVA ou PF-127, e é agitada durante uma hora até o solvente orgânico evaporar. De seguida, as partículas são centrifugadas duas vezes para remover o excesso de tensioativo e no final, resuspendidas em PBS pH 7.4.

Procedeu-se à caracterização das propriedades físico-quimicas destas NPs, como o diâmetro médio, a distribuição de diâmetros médios, carga à superfície e morfologia das NPs constituídas por PLGA-PEG, PLA/PLGA-PEG e PLA/PLGA-PEG-Manose. Todas estas NPs mostraram terem características que lhes permitem ser internalizadas pelas DCs, com um tamanho inferior a 200nm e com uma morfologia esférica. Porém, apresentaram uma carga superficial negativa. Estas NPs mostraram não alterar a viabilidade da linha celular de células dendríticas imaturas (JAWSII), quando incubadas numa concentração até 1 mg/mL. Estas NPs foram internalizadas pelas DCs *in vitro*, ainda que com diferentes taxas de internalização, sendo a NP composta por PLGA-PEG a menos internalizada.

A segunda parte deste projecto de investigação consistiu em investigar de que modo o revestimento das NPs com PEG interfere na internalização e maturação das DCs *in vivo*. Com base nos dados anteriormente obtidos, produziram-se NPs com PLA, nomeadamente PLA/PLGA, PLA/PLGA-Manose e PLA/PLGA-PEG-Manose.

Novamente procedeu-se à sua caracterização físico-química tanto de NPs vazias (sem antigénio e adjuvantes) como de NPs contendo os adjuvantes oligodeoxinucleótidos de CpG não metilados (Cpg) e ácido poliinossínico:policictílico (Poly (I:C)), e neo-antigénios expressos em células tumorais de melanoma e glioblastoma.

Todas as NPs produzidas apresentaram propriedades físico-químicas adequadas para a sua internalização pelas DCs, com tamanho médio perto de 200 nm e distribuição estreita de tamanho de partícula. Todas as NPs incorporaram quantidades de neo-antigénios de glioblastoma ou melanoma, e dos adjuvantes CpG e Poly (I:C) adequadas às necessárias para

a atividade biológica pretendida. Assim sendo, estas NPs reúnem as características que prevêm a sua utilização na estimulação de uma resposta imune forte e duradoura especificamente induzida contra estes tumores cerebrais.

Quando estudada a internalização das NPs e ativação das DCs *in vivo*, todas as NPs foram mais internalizadas por DC migratórias. Todas as NPs induziram com sucesso a maturação das DC migratórias, com o aumento da expressão das moléculas co-estimulatórias MHC que são essenciais para a apresentação de antigénios e ativação das células T.

Palavras chave: Células apresentadoras de antigénios (APC), neo-antigénios, adjuvantes, vacinas, tumores cerebrais

Acknowledgements

I wish to express my gratitude, firstly, to everyone of the BioNanoSciences, drug delivery and Immunotherapy unit of the INETI who helped me in this work, specifically Ana Matos and Bárbara Correia. These PhD students provided me continuous direct day-to-day support and helped me in all the steps of the project, which included fluorescence analysis, NPs synthesis and DCs maturation assay. I am thankful to Liane Moura, an excellent professional that shared her expertise on NPs formulation and for integrated me in the lab group.

I am especially indebted to PhD Helena Florindo for giving me the suggestion to study this important pathway in cancer immunotherapy and for always being available to help me. I also have to thank to João Conniot for the scientific input into this work, to push me to develop critical thinking and for the writing guidance in this project.

I would like to thank all the people who contributed to the realization of my master degree. Inês Pais, Ana Margarida Tomé, Ana Coxixo and Miguel Guedes for making me laugh when all I wanted was to cry. I am also thankful to my lab colleagues namely Mariana Mateus, Filipa Gonçalves and Sandra Pena for helping me overcome the obstacles and celebrate the achievements. I also want to thank Inês Raposo for her patience in explaining me how GraphPad Prism 8 can be used to its potential.

To Tiago Portela I also owe a word. His unreserved support, patience and love were really important in this journey. Thank you for always being one phone call away.

Finally I want to acknowledge my parents, who gave me the conditions to carry out the Master in Biopharmaceutical Sciences.

Table of Content

List of abbreviations

APCs – Antigen presenting cells
ANOVA – Analysis of variance
AuNPs – Gold Nanoparticles
BBB – Blood Brain Barrier
BCRs – B cells receptor
CLR – C-type lectin receptors
CMC – Critical micelle concentration
CNS – Central nervous system
CpG – Unmethylated CpG oligodeoxynucleotides (CpG)
CTL – Cytotoxic T cells
CTLA-4 – Cytotoxic T-lymphocyte–associated antigen 4
DCs – Dendritic cells
iDCs – immature dendritic cells
DCM – Dichloromethane
ECs – Endothelial cells
EE – Entrapment efficiency
ER – Endoplasmic Reticulum
EPR – Enhanced permeability effect
GBM – Glioblastoma Multiforme
HIF – Hypoxic factor
HLB – hydrophilic-lipophilic balance
IFN – Interferons
IL – Interleukin
LNs – Lymph nodes
MDSC – Myeloid derived suppressor cells
MHC – Major histocompatibility complex
NK – Natural killer
NPs – Nanoparticles
PdI – Polydispersity index
PD-1 – Programmed cell death-1
PEG – Polyethylene glycol
PEO – Polyethylene oxide

PLA – Poly(lactic acid)

PLGA – Poly(lactic-co-glycolic acid)

PGA – Poly(glycolic) acid

Poly (I:C) – Polyinosinic:polycytidylic acid

PPI – Poly(propylene imine)

PPO – Poly(phenylene oxide),

PVA – Poly(vinyl acetate)

RES – Reticuloendothelial system

TAAs – Tumor associated antigens

TAM – Tumor associated macrophages

TAP – Transporter associated with antigen processing

TCR – T cells receptors

Th cells – T helper cells

TLR – Toll-like receptors

TME – Tumor microenvironment

TPGS – d-α-Tocopheryl polyethylene glycol 1000 succinate

Treg – Regulatory T cells

VEGF – Vascular endothelial growth factor

VLP – Virus-like particles

List of figures

List of tables

Chapter 1 – Introduction

1.1 Cancer and the dysregulation of the immune system

The changes in the regular function of the immune system and how they affect cancer initiation and progression have been one of the most intriguing subjects of discussion over the past years in cancer research, since it is the most fatal disease worldwide with more than 11 million deaths being expected in 2030[2].

Malignant brain tumors affect 7 per 100,000 population in Europe and these numbers are expected to increase due to combinations of genetic mutations and environment factors, including ionizing radiation and toxic agents (nitrosamide). Common symptoms include coordination and cognitive perturbations[3,4].

Brain tumors can be divided into various types based on their nature – benign or malignant –, and origin – primary or secondary. According to the World Health Organization (WHO), tumors can be further categorized in four grades based on their rate of growth and by their progression stages in a scale from 0 to 4. Stage-0 refers to abnormal tumor cells that have not spread, while stage-4 relates to tumor cells spreading throughout the body[4].

Glioblastoma (GBM) is the most frequent and aggressive primary cancer of the central nervous system (CNS), with an incidence of 3–5 out of 100,000 individuals in Western countries. Each year, about 240,000 cases of brain tumor are diagnosed worldwide, of which the majority are GBMs. GBM arises either *de novo* (primary GBM) or develops from a lower grade astrocytom (secondary GBM). Primary and secondary GBMs are histologically indistinguishable, yet they show distinctive genetic alterations that can allow for differentiation. For example, using genome sequencing techniques and transcriptional analyses of patients' tumors, genetic alterations involved in primary GBM have been identified such epidermal growth factor receptor (EGFR) amplification and phosphatase and tensin homolog (PTEN) deletion or mutation. Patients with a clinical diagnosis of secondary GBM are on average 17 years younger than those with primary GBM, affecting people below the age of 45[5].

Other type of tumor that can be found in brain region is metastatic melanoma, with an incidence of 2.8–3.1 per 100,000, with median overall survival from diagnosis of brain metastasis in the range of 17–22 weeks[6,7]. Despite the mechanisms underlying tumor growth remain unclear, it is known that ultraviolet (UV) radiation and environmental factors can trigger the transformation of melanocytes into cancer cells (melanoma initiation)[8]. Besides

environmental factors, genetic mutations in the JAK/STAT3 and PI3K/AKT/mTOR pathway have been identified. Depending on the metastases location, the mutations in JAK/STAT3 and PI3K/AKT/mTOR pathway are different[9].

When diagnosed at early stages, i.e. when tumor cells have not reached the lymph nodes (LNs), melanoma can be easily resected. However, when the malignant cells have spread from its site of origin to another part of the body, such as brain, lungs, and liver, metastatic melanoma become highly resistant to the available therapies, including chemotherapy and radiotherapy. Indeed, half of melanoma deaths is related to melanoma brain metastases[10].

Current brain tumor treatments include brain radiation therapy, stereotactic radiosurgery and surgical resection followed by temozolomide treatment, an oral alkylating agent used in chemotherapy for brain cancer. Surgical removal of cancer cells is difficult, time consuming and painful. Since conventional chemotherapy it is not target specific, the healthy cells are affected and therefore, severe side effects may happen. In case of radiation therapy, where external near infrared radiations (NIR) is converted into heat to destroy tumor cells some major drawbacks can be pointed out such as uneven penetration of heat into tumor cells and the lack of efficiency on removing tumor cells[11,12].

Nevertheless, tumors develop high resistance to the treatment and tumor recurrence is frequent. This condition leads to a 5-year survival rate below 5%, being the mean survival around 14 months in GBM and 17 months for metastatic melanoma[6,12,13]. In cases where tumors no longer benefit of curative therapy, the focus shifts to life prolonging treatments with systemic chemotherapy[14].

Under physiological conditions, the immune system modulates tumor growth and immunogenicity in a process named cancer immunoediting. This process has been illustrated through three stages: elimination, equilibrium and escape, leading to uncontrolled proliferation[2,15].

As validated with genetically modified mouse models lacking immune effector cells, the immune system has a crucial role in protecting our organism by recognizing exogenous pathogens and fighting against them, without affecting self-tissue[16].

As dendritic cells (DCs) localize in the peripheral tissues (skin and mucosal surfaces), close to the main pathways for pathogen access, DCs are considered to be professional antigen-presenting cells (APCs) responsible to identify self and non-self molecules as bacteria and viruses to trigger an immune response. Non-activated DCs present an immature state (or steady state), in which they regulate adaptive immune cells, such as T and B cells, preventing them from attacking the host cells, maintaining immune tolerance[17].

DCs recognize malignant, dying, or stressed cells, internalizing them through phagocytosis, and if successful, these become activated and migrate to lymphoid tissue where a secondary immune response will be generated[18].

In the process of internalization, the endocytic vesicle containing tumor antigen enters the cytoplasm, where it fuses with an early or sorting endosome. Within the lysosomal compartment, antigens are degraded to small peptides and form a stable major histocompatibility complex (MHC) class II-peptide complex that is further transported to the DCs cell surface. After that, the MHCII-antigen complex is presented to $CD4^+$ T cells (Figure 1).

An alternative T cells presentation pathway designated cross-presentation has been described, in which APCs can acquire both tumor antigens and cell-associated antigens and further present them to MHC class I molecules (MHCI). After those antigens enters into the cytoplasm, where it fuses with an early or sorting endosome, antigens escape from the endosome. Later, cross-presentation requires antigen to be processed by the cytosolic-based proteasome into small peptides and transported from the cytoplasm into the endoplasmic reticulum (ER) *via* the transporter associated with antigen processing (TAP). In the ER they associate with MHCI. This mechanism insures the activation of $CD8^+$ T cells, which is highly relevant for anti-tumor vaccines[17,19].

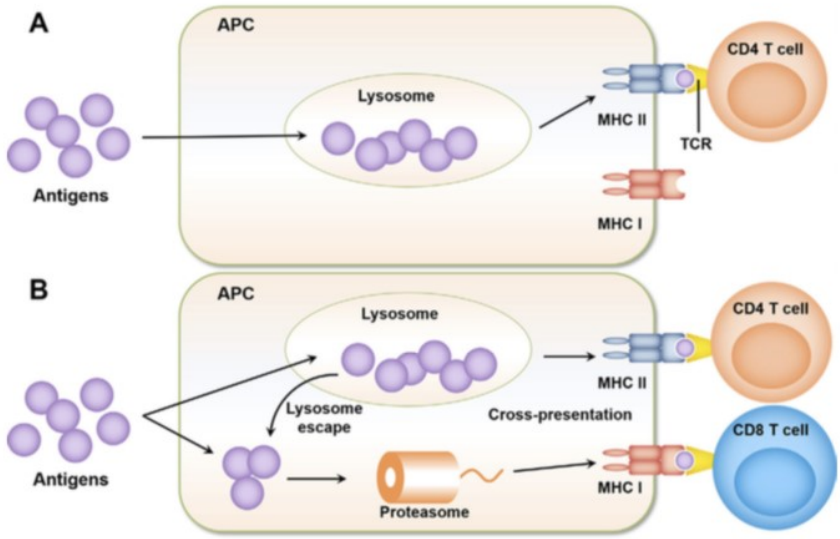

Figure 1 Schematic illustration of exogenous antigen presentation mediated in different ways. A) Classic presentation of exogenous antigens via MHC II molecules. B) Cross-presentation of exogenous antigens via MHC I. As the professional antigen-presenting cells, DCs are able to capture, process and present both exogenous antigens and

endogenous antigens. In the classic antigen presentation, exogenous antigens are degraded into oligopeptides and then presented by MHC-II molecules to the surface of DCs for recognition of CD4 T cells; while in the cross presentation mechanism, the exogenous antigens are processed by cytoplasmic proteasomes and then presented by MHC- I molecule to the surface of DCs for recognition of CD8 T cells[20].

Besides the expression of the MHC complex on DC surface, DCs also needs to express costimulatory factors like CD80/86 and CD40 that will interact with CD28 and CD40L (CD154) receptors on the T cell surface. Along with interleukin (IL)-12 release, DCs become mature and capable of effectively present and activate naïve T cells[21].

Once the maturation process is complete, DCs migrate to the draining lymph nodes (dLNs) to present antigenic peptides to naïve T cells, initiating adaptive immunity[22]. After the recognition of the MHC-antigen complex by the T cells receptors (TCR), $CD8^+$ T cells differentiate into cytotoxic T lymphocytes (CTLs). Meanwhile $CD4^+$ T cells differentiate into T helper cells (Th cells) Th1, Th2, Th17 and regulatory T cells (Treg), according to specific cytokines (IL-12, IL-4, IL-1/IL-6/IL-21, and TGF-β, respectively) and TCR affinity towards the antigen[21,23]. IFN-γ-secreting Th1 cells promotes macrophages and neutrophils recruitment into the infection site, resulting in enhanced phagocytic activity[19].

CTLs are responsible for mediating tumor cells killing through four main pathways: i) perforin produced by effector T cells and NK cells creates an extracellular membrane pore in the tumor cells, to facilitate granzyme B access to caspases, ii) binding of Fas-ligand (FasL) with its receptor on tumor cells, resulting in the activation of a caspase cascade, iii) interaction of TNF-related apoptosis-inducing ligand (TRAIL) expressed on activated T cells and NK with TRAIL receptors found on tumor cells and iv) through interferon-gama (IFN-γ) release from T cells and NK cells. All these processes culminates with cell apoptosis[24].

In the apoptotic process, caspase molecules (3 and 8) are activated and start to cleave important cellular proteins (nuclear, cytoskeletal and DNA repair proteins), which contribute to cellular apoptosis morphological features. These morphological changes includes round shape, reduction of cellular volume and retraction of pseudopodes[25].

After the primary immune response, a quicker and stronger immune response is generated. In the secondary immune response, effector T cells undergo expansion and contraction and acquire memory, with 90-95% of lymphocytes undergoing apoptosis during contraction and the remaining 5-10% differentiating into memory T cells[26]. Different memory

T cell populations have been described, some of them recirculating between lymphoid organs and others being present at peripheral tissues[27].

B cells also sense antigens, but instead of recognizing them by the TCR, antigens are internalized through B-cell receptors (BCRs). These antigens are then loaded in MHCII molecules and, after the combination of CD40L molecule on the Th cell membrane with CD40 molecule on the B cell membrane, B cells became activated promoting the release of antibodies (humoral immunity). These antibodies neutralize pathogen aggression or activate phagocytic cells (e.g macrophages) to promote maintenance of memory for long periods of time without a constant stimuli[28]. Hence this immunological response guaranty a rapid and effective response to foreign antigens that have been previously encountered[28].

However, apoptotic pathway does not always occur as tumor cells modulate the function of suppressor immune cells, which favors tumor evasion[16].

1.2 Cancer immune evasion mechanisms

Cancer initiation and progression is the result of multiple genetic changes during which healthy cells are transformed into tumor cells. These genetic alterations can be induced by radical oxygen species (ROS) from mitochondrial respiration, errors during DNA replication, UV light and ionizing radiations, among others. Both the endogenous and exogenous factors may produce mutations in the DNA sequence as well as epigenetic alterations, at the chromosome level. Most likely both chromosomal derangements and mutations promote tumor initiation[29,30]. One mechanism underlining tumor initiation is angiogenesis.

During normal tissue development, angiogenesis is extremely important to provide continuous supply of oxygen and nutrients[31]. Depending on the cell type and the organism, cell size varies between 10-100 μm. However in pathological conditions, tumors can reach few millimeters where the amount of oxygen and nutrients are not sufficient to support tumor growth[32].

With the continuously amount of oxygen being increasingly lower, tumor cells release hypoxia-inducible factors (HIFs) that mediate pro-angiogenic factors transcription molecules, including vascular endothelial growth factor (VEGF). The resulting proteins can trigger a metabolic switch, from oxidative phosphorylation to aerobic glycolysis and can induce "angiogenic switch" to increase oxygen delivery required for their high energy demand and growth. Pathological angiogenesis is an extension of vasculogenesis, which involves the development of leaky blood vessels from pre-existing vessels, being characterized by abnormal morphology and structure[31,32]. By releasing cytokines, growth factors and interleukins, tumor cells can stimulate the degradation of extracellular matrix (ECM), where the resulting endothelial cells (ECs) migrate towards tumor tissue to form blood vessels along with pericytes**.** Since blood vessels irrigate cells with oxygen and nutrients, it allows tumor growth, proliferation and dissemination to distant sites, where they can develop a secondary tumor and perturb critical function of that organ[33,34].

Another feature of VEGF is its capacity to downregulate integrins' expression, when overexpressed, instead of regulating cell–to–cell communication, maintaining the overall homeostasis[35]. As shown in solid cancers, including melanoma and renal cell carcinoma, the expression of endothelial adhesion molecules, such as intracellular adhesion molecule (ICAM–1) and vascular cell adhesion molecule (VCAM–1) are impaired upon VEGF binding, which ultimately blocks ECs – lymphatic ECs interaction[36]. Subsequently, the migration of APCs from peripheral tissues towards LNs and central circulatory system is limited, and thereafter

antigen presentation to T cell and immune response will be compromised. Indeed, lymphatic vessels have been shown to be actively involved in tumor progression. In agreement with this, two studies found that lymphatic dysfunction or absence of lymphatic vessels led to limited tumor-associated antigens transport to LNs and reduced T cell activity in B16F10 melanoma model, which was followed by reduced tumor inflammation, reduced immune cell infiltration at the site of the primary tumor, and increased tumor growth[33,37].

Apart from influencing ECs, VEGF mediates the development and accumulation of immunosuppressive immune cells (myeloid-derived suppressor cells (MDSCs), tumor-associated macrophages (TAMs) and tumor associated neutrophils (TANs))[32,33].

With increasing immunosuppressive cells within the TME and their respective cytokines, tumor cells downregulate several immune cell subpopulations and modulate cell polarization (e.g M2-TAMs phenotype)[33]. M2-like TAMs secrete several cytokines, such as IL-1, IL-6, IL-10 and TGF-β that play different roles in cancer development, promoting maintenance of iDCs phenotype and converting $CD4^+$ T cells into immunosuppressive Treg cells, which suppress CTL-mediated responses leading to tumor proliferation[2,33]. Altogether the levels of VEGF, MDSCs and TAMs in the blood are related to tumor progression, which can be correlated with cancer patients' poor prognosis[38].

Other strategies to evade immunosurveillance is the upregulation of proteins that increase resistance to apoptosis (Bcl2, p53) and expression of immune checkpoint inhibitors to promote tumor survival[25].

Immune checkpoints refer to all the signaling pathways involved in the regulation of an immune-mediated elimination response of tumor cells[39]. As elucidated before, CD80 and CD86 molecules engage with CD28, promoting T cell activation. Yet cytotoxic T lymphocyte–associated antigen 4 (CTLA-4, or CD152), a protein receptor found in T cells has higher affinity towards CD80 and CD86 molecules than CD28. As a consequence, upon CTLA-4 and CD80 and CD86 molecules engagement, a negative costimulatory signal prevents naïve T cell activation[15,16].

Another negative regulator of immune response is programmed cell death 1(PD-1). The continuous exposure to tumor-associated antigens (TAAs) and the release of IFN-γ produced by TAA-specific T cells within the TME, induce PD-1 expression on reactive T lymphocytes and up-regulates PD-L1 in APCs and tumor cells. PD-1–PD-L1 engagement blocks TCR signaling, which inhibits $CD4^+$ T cell activation and its proliferation and decrease effectiveness of CTL cells and thereby restricting tumor cell killing (T cell exhaustion)[40]. As this state of

exhaustion is characterized by the reduced cytokine production (IL-2, IFN-γ) and a defective memory T cells, it allows tumor cell evasion and cancer progression[41].

In brain tumors, tight junctions in vascular ECs (ZO-1, claudins and occludins), integrins (α3β1, αvβ3 and α4β1) and proteases (MMP-9) are deregulated[9]. In normal conditions, the ECM has essential signals that support cell development, migration, adhesion, proliferation and overall cell–cell communication. When the tumor hypoxic factors downregulate the molecules involved in those processes, instead of acting as a barrier among tumor cells, those same factors can facilitate cell invasion from the systemic circulation to brain vasculature[34].

For many years the mechanisms that underlie the migration of melanoma cells into the brain have remained unclear. Metastasis is a complex, multi-step process resulting in the spread of tumor cells from a primary lesion to the surrounding tissue and later to blood circulation to move passively through the blood brain barrier (BBB), to brain vasculature that results in increased patient morbidity and mortality[9,42].

Once melanoma cells reach the brain, tumor cells interact with healthy brain cells, specifically with the brain-resident macrophages (microglia) and with astrocytes. In normal conditions, astrocytes are responsible for regulating brain homeostasis with action in ionic balance, pH, metabolism, and the integrity of the BBB. Nevertheless, in contact with tumor cells, they become activate (reactive astrocytes) contributing to tumor survival through the release of IL-6, TNF-α, IL-1β, growth factors and also by regulating drug resistance machinery[9].

The resultant malignant cells are characterized by uncontrolled proliferation, resistance to cell death mechanisms, capacity to invade and to modulate the local microenvironment[32]. Altogether tumor cells drive a chronic inflammatory and suppressive TME through the release of soluble factors[33].

Since the CNS is protected by blood-brain barrier (BBB, a physiologically active barrier between brain parenchymal vasculature and brain parenchyma); the blood-meningeal barrier (BMB, a cellular barrier between the meningeal blood vessels and the meninges), and the blood-CSF barrier that prevents blood moieties from entering to the ventricular CSF), peripheral molecules are inhibit from entering the brain parenchyma[43].

In this sense, all the physical barriers mentioned above impact CNS delivery, there is an urgent demand for designing new, effective and specific molecules capable of overcome all this obstacles to attempt CNS assessment at therapeutic concentration[44].

1.3 Cancer Immunotherapy

Immunotherapy has been an emerging alternative therapy for brain tumors, such as GBM and brain metastases, where the main principle is re-activating host's immune system to attack tumor cells[18]. Through modulations of the immune system, it is possible to take advantage of the immune system capacity to acquire memory to prevent further recurrence, leading to better outcomes in brain cancer[43]. With cancer immunotherapy, activated and tumor-specific immune cells can reach areas where the surgeon cannot and due to its specificity, side effects of chemotherapy and radiotherapy can be avoided. Immunotherapy should be considered for cancer treatment as it can directly target the tumor and its microenvironment. Within immunotherapy strategies, it is important to highlight the performance of monoclonal antibodies (mAbs) and vaccines[45].

mAbs are artificial versions of large proteins produced by B-cell clone, which have unique antibody-binding fragments that allows them to bind to epitopes on the cancer cell. There are several classes of immunoglobulin that differ on the basis of size, charge, amino acid composition, and carbohydrate content, being the IgG antibody the most abundant class[46].

Important mechanisms used by mAbs to kill targeted tumor cells are i) inhibition of both growth factor ligands and its receptors that are activated in angiogenesis ii) antibody-dependent cell mediated cytotoxicity (ADCC) and iii) complement-dependent cytotoxicity (CDC). Firstly, antibodies bind to tumor antigens and then, as the Fc receptors expressed on macrophages and natural killer (NK) recognize tumor antigen bound to the mAbs, it mediates tumor cell apoptosis through perforin and granzyme cytotoxic agents. CDC mechanism involves antibodies and tumor antigens engagement, in which a complement cascade is induced with other complement binding to the antibodies. These binding triggers a membrane attack complex (MAC) leading to tumor cell lyses[45].

Immune checkpoints are the mainly target for mAbs. Most of the immune checkpoints, defined as a set of immune inhibitory pathways, are essential to preserve the quality and amplitude of physiological immune responses. However, in pathological conditions, both inhibitory ligands and T-cells receptors (CTLA-4 and PD-1) are overexpressed, where their engagement compromises CTL function. In this context, blocking immune checkpoint receptors is crucial to potentiate anti-tumor immune responses and eliminate tumor cells and thus, in enhancing the effectiveness of the immune system[47].

As mentioned before CTLA-4 regulates the activation of T cells and therefore T cell-mediated pathway can be activated by blocking the interaction between CTLA-4 and its ligands. So, blocking CTLA-4 with mAbs such as Ipilimumab and Tremelimumab, approved by the FDA for patients with advanced melanoma, is associated with enhancement of T cell responses and tumor elimination[47].

The PD-1 receptor present on activated T cells has also emerged as a promising immunotherapy target. In chronic infections, PD-1 engagement with PD-L1 or PD-L2 leads to CTL exhaustion, resulting in decreased T cell proliferation and cytokine production and further ineffective tumor elimination. Blockade of PD-1-ligands with mAb has been found to enhance T cells responses, by restoring exhausted $CD8^+$ T cells function. Moreover, *in vivo* administration of anti-PD-L1 antibody increased both $CD4^+$ and $CD8^+$ T cells. Nivolumab and Pembrolizumab both for melanoma tumors, are examples of humanized antibody used in cancer immunotherapy[41,48].

It has been reported that immune cells associated with both innate and adaptive immunity have the ability to pass through the BBB, as this physical barrier is partially deteriorated in glioma. In this sense, the discovery has led to consider the CNS immunologically distinct rather than privileged[13,49].

As DCs are considered to be professional APCs once they can develop antigen-specific responses through $CD4^+$ and $CD8^+$ T cells, targeting DCs is a promising approach[18]. With this, it is expected to eliminate tumor cells or controlling their overall expansion, delaying tumor recurrence and prolonging survival[50]. Cancer vaccines are another available immunotherapeutic treatment that is going to be further discuss here.

1.4 Cancer vaccines as an immunotherapeutic strategy

1.4.1 Neo-antigens

The importance of antigen recognition in mediating CTL immune responses has led to an extensive TAA characterization[2]. TAAs can be divided into two categories, self-antigens and neo-antigens, also referred as tumor specific antigens. Self-antigens are non-mutated peptides expressed in cells and overexpressed in tumor cells[51]. On the other hand, neo-antigens are peptides that result from post-translational modifications or somatic tumor mutations and thereby may be recognized in a different way[32].

The use of self-antigens expressed in normal and tumor cells may explain the poor results of tumor vaccines in the past, by a reduction of immunity due to central and peripheral tolerance[52]. To efficiently address these challenges, the investigators turned their attention to neo-antigens. Due to neo-antigens' strong immunogenicity and since they are exclusively expressed by the malignant cells, they constitute an important target for tumor immunotherapy with the benefit of destroying developing cancers before they become clinically relevant[15,32].

Here, we will focus on GBM and metastatic melanoma neo-antigens due to the emergence in finding new and effective treatment to primary and metastatic brain tumors. Indeed, neo-antigens have been reported to induce anti-tumor response *in vivo* with $CD8^+$ and $CD4^+$ T cells responses[53]. In fact, two neo-antigens against GBM demonstrated to increase T cell infiltration, passing from the peripheral blood into the brain, and enhanced patients' median total survival time to 29 months[53].

Discovering a potential neo-antigen depends on different key steps: i) whether the somatic mutation can be translated into a protein, ii) whether the mutant protein can be processed and become available to form complexes with MHCI/II molecules and iii) whether the mutant peptide-MHC complex has affinity with TCR[54].

To identify neo-antigens, comparing tumor and non-mutated sequences is required. Somatic tumor mutations like indels or frame-shift mutations change the amino acid sequences and spatial structure. So the mutant sequence that it is going to be recognized by T cells will be different from the non-mutant peptide[54]. Therefore, cancer patients' DNA and RNA exome should be sequenced to predict neo-antigens. In addition, as the mutant peptide has a stronger affinity towards MHC, *in silico* computational approaches could also be used to predict their

affinity, once they are more likely to be recognized as a neo-antigen by T cells[53].Yet, it is important to highlight that the amount of mutations cannot be correlated with tumor immunogenicity, since an immunosuppressive TME and defective antigen presentation machinery may lead to an insufficient tumor-specific immune response[32].

Since tumor neo-antigen T cell responses are hard to find and neo-antigen candidates hard to predict, validation tools must be optimized to ensure that the right immunogenic neo-antigen is predicted[54,55]. Another associated challenge is the development of an effective delivery system carrying an universal neo-antigen that could be used in any cancer to trigger T cell responses[55].

Upon neo-antigen design and recognition, CTL can selectively target and destroy malignant cells presenting epitopes that have been recognized. However, their isolated response is often not enough to kill tumor cells. Neo-antigens *per se* have failed to reach their therapeutic potential due to insufficient delivery to the lymphoid tissues caused by their highly susceptibility to enzymatic degradation upon systemic administration and low membrane permeability. Entrapping neo-antigens in nanocarriers may help overcoming biodistribution and bioavailability issues. However, even within a nanocarrier, neo-antigens proved to be poorly immunogenic and weak antigenicity, requiring multiple administration[2,56].

Hence, the development of an efficient cancer vaccine seems to be dependent on TAAs together with adjuvants, to effectively stimulate CTL and Th cells responses towards a tumor epitope. Indeed, combinations of melanoma antigens against both MHCI and MHCII with two adjuvants in nanoparticles (NPs), have demonstrated to produce a stronger cytotoxic activity compared to the NPs containing only the antigens, suggesting the importance of the activation of the adaptive immune cells for the efficacy of the anti-tumor immune response. Thus, adjuvants are being considered to boost the immune system[57].

1.4.2 Adjuvants

The generation of an effector T cell response requires the presentation of peptide/MHC and costimulatory molecules for T-cell activation (Figure 2). Peptide-based antigens require an adjuvant to generate danger signals such as the presence of Toll-like receptors (TLRs) and C-type lectin receptors (CLRs) agonists[58]. Effective adjuvants enhance anti-tumor immunity by inducing Th1 downstream signalling cascade, culminating in the activation of DCs, $CD4^+$ and $CD8^+$ T cells[59].

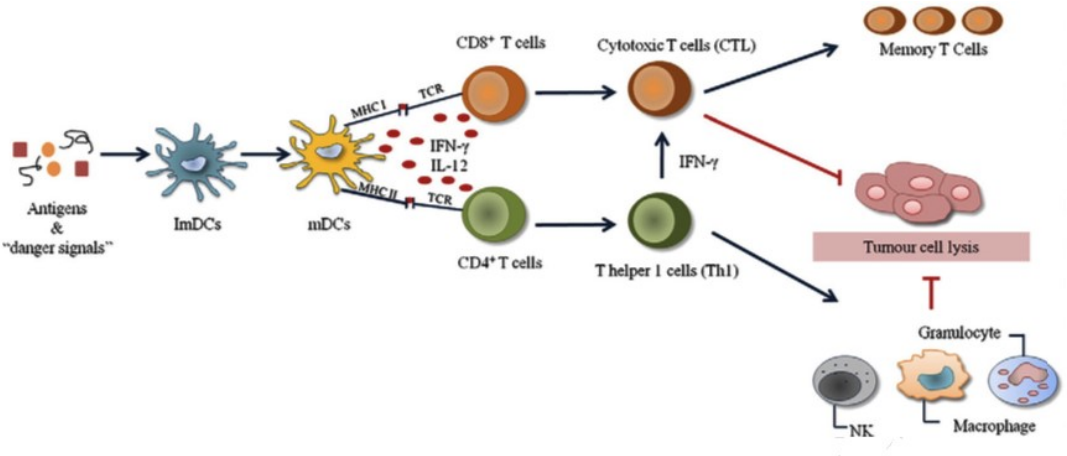

Figure 2 Desired immune response elicited by a therapeutic cancer vaccine: tumor antigens and cell-associated antigens are internalized by immature dendritic cells (iDCs). After processing, the resultant peptides will be loaded onto major histocompatibility complex (MHC) class I or MHC class II on DCs surface. Simultaneously, "danger signals" promote the activation and maturation of DCs, which consequently express costimulatory molecules and secrete cytokines (INF-γ and IL-12), which stimulate activation and differentiation of both $CD8^+$ and $CD4^+$ T lymphocytes. $CD4^+$ to T helper cells 1 (Th1) and $CD8^+$T cells into cytotoxic T lymphocytes (CTL). Some of these cells acquire memory phenotype, which is crucial for the maintenance of immunity whereas Th1 cells enhance the action of CTL by maintaining memory phenotype and promotes recruitment of cells from the innate immune system, such as the natural killer (NK) cells, granulocytes or macrophages that also contribute to tumor cell lysis. Adapted from[19].

One study carried by Warger *et al.* (2006) revealed the induction of $CD8^+$ and $CD4^+$ T cells response when combining TLR3 and TLR7 ligands. Besides overcoming Treg immunosuppressive function, this synergy elicited a faster pro-inflammatory cytokine release and expression of costimulatory molecules, which induced an increase of CTL expression in

wild-type mice *in vivo.* However, not all the combinations of TLRs have positive outcomes. If we take the example of the combination of TLR2, 4 and 5, instead of decreasing Treg activity, it enhances their suppressive function. Zoglmeier *et al.* (2011) also claimed that TLR could modulate MDSCs function in tumor-bearing mice[19].

According to the subcellular localization, TLRs can be divided into two subfamilies. TLR1, 2, 4–6, 10 in humans and TLR11 in mice, expressed on plasma membrane at the cell surface, can recognize lipids[22.]. TLR3, 7–9 localized on the endosomal membrane of immune cells, detect nucleic acids from the extracellular environment[59].

One example of an adjuvant is the TLR9 ligand, the unmethylated CpG oligodeoxynucleotides (CpG). CpG is a synthetic molecule mimicking a danger signal that acts as an immunostimulatory alarm, being easily detected by TLR9 in the endosomes. By targeting TLR9, CpG upregulate costimulatory molecules, activates DCs maturation and facilitates antigen cross-presentation, which triggers a specific and long-lasting pro-inflammatory cytokine production (TNF-α and IL-10). Furthermore it triggers the downregulation of Treg and MDSC immunosuppressive phenotype[19,59,60].

Zheng and colleagues (2008) claimed that the synergy between CpG and a TLR3 ligand was required to obtain significant tumor regression, demonstrating the advantages of combining adjuvants in cancer vaccination trials. The co-adjuvant used in his study was the double stranded (dsRNA) polyinosinic:polycytidylic acid (poly I:C)[61].

Poly (I:C) is a TLR3 ligand expressed in the endolysosomal compartment of DCs, NK, T cells and macrophages. Poly (I:C) can also bind to melanoma differentiation-associated protein 5 (MDA-5) and retinoic acid-inducible gene 1 (RIG-I) found in the cytoplasmic receptors of macrophages and neutrophils[61].

Because this TLR3 ligand can also activates others non-immune cells, it might induce immune tolerance since it increase the self-antigen presentation rate[59].

As shown in several types of tumor cells, including breast cancer and colon carcinoma, Poly (I:C) ligation induced a strong Th1 and cytotoxic response through type I IFN (IFN-α and IFN-β) secretion[62]. The release of both IFN and Th1 specific pro-inflammatory cytokines with costimulatory molecules expression, induces CTL activity and antibody release, which together primes tumor apoptosis[59].

2. Anticancer vaccine delivery system

So far we have been discussing the importance of selecting an immunogenic antigen, exclusively expressed in tumor cells and combinations of different TLRs ligands on NP surface to increase the effectiveness of the immune response. Delivery of free antigens and adjuvants alone to APCs is insufficient to induce immunity, due to their susceptibility of enzymatic degradation upon systemic administration. In this regard, many studies have focused on using immunogenic antigen-delivery platforms, like NP-based delivery systems, to delivery antigens and adjuvants. To ensure a potent immune response, the vaccine platform must effectively lead to the recruitment of APCs and antigen uptake, further maturation and migration to LNs to induce T cell activity. Lee *et al.* (2018) reported that if one of these criteria is not fully accomplished, the cancer vaccine will not be effective[2,51].

The use of nanotechnology in immunotherapy has demonstrated several advantages because it can improve the solubility of poorly water soluble drugs, enable a slow release of antigens and adjuvants into APCs, increase drug bioavailability, increase NP specificity towards APCs, thereby reducing frequency of administration. Additionally with this approach, the risk of T-cell exhaustion is minimized and patient compliance improved[2,63,64].

A diversity of nanocarriers raging between 1–1000 nm has been used for the delivery of broad molecules, such as genes and biomolecules. The nanocarriers can be classified based on the material used: lipids (e.g liposomes), polymers (e.g NPs, dendrimers, and micelles), proteins (e.g VLPs) and inorganic carriers (e.g gold nanoparticles) (Figure 3)[65]. These nanocarriers can be prepared with different formulation processes to have certain morphology, size and chemical properties that will dictate the biodistribution, accumulation and elimination of NPs and overall therapeutic effect[63,66].

Due to the facility of producing NPs with various sizes and shapes, NPs have also been investigated for integrating diagnostic and therapeutic agents, enabling their application on monitoring the biodistribution and target site accumulation, visualizing and quantifying drug release and assessing the therapeutic efficacy[67].

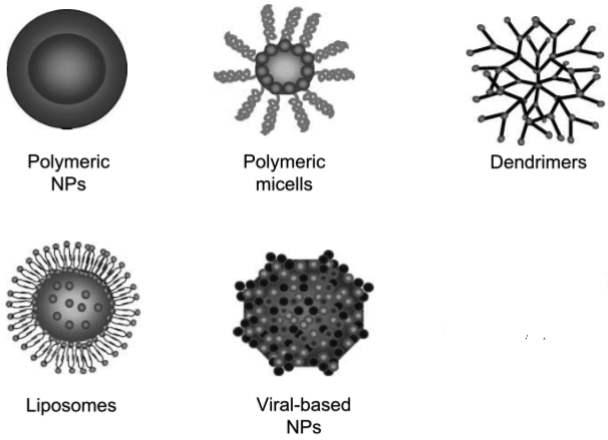

Figure 3 Types of nanocarriers for drug delivery. Adapted from[68].

2.1 Liposomes

Liposomes consist on an aqueous core surrounded by phospholipid bilayers and cholesterol. This unique property enables the incorporation of both hydrophilic and hydrophobic therapeutic molecules: hydrophilic molecules are incorporated within the aqueous compartment, while the hydrophobic ones are entrapped within the hydrophobic long tails. Due to their composition, liposomes are more biocompatible than other synthetic materials, being capable of crossing lipid bilayers and cell membranes, and delivering drugs to APCs in a slow manner. The presence of cholesterol and rigid saturated lipids in their constitution allows liposome stabilization towards extracellular insults, protecting the entrapped drug from degradation. In order to release the therapeutic drug from the liposome, ultrasound, enzymes and light can be employed[2,69].

However, the entrapment of small hydrophilic molecules has been difficult once they can aggregate or even escape from the liposomes during lipid phase state transition when stored[2,70].

2.2 Polymeric micelles

Polymeric micelles are formed by block-copolymers consisting of hydrophilic and hydrophobic monomer units, in which their structure assembled to form spherical nanocarriers (Figure 4). The hydrophilic and hydrophobic monomer units can be displayed into two conjugated blocks each consisting of monomers with the same hydrophobicity (A-B-type copolymers), or can form alternating blocks with different hydrophobicity (A-B-A-type copolymers)[71]. The most commonly used hydrophilic block is poly(ethylene oxide)/poly(ethylene glycol), PEO/PEG[72].

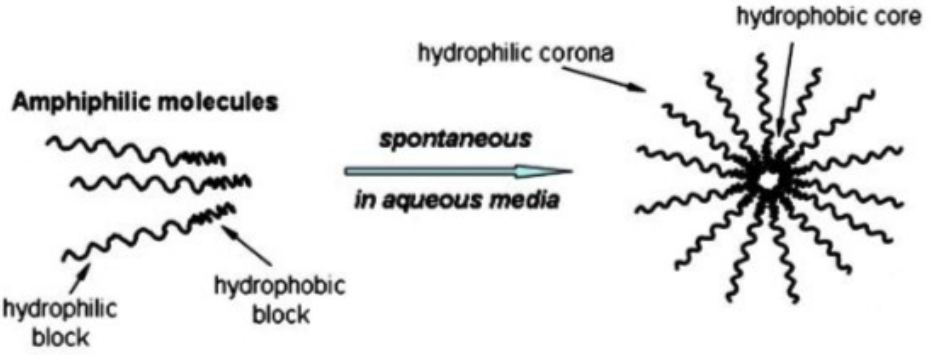

Figure 4 Spontaneous micelle formation from amphiphilic molecules in aqueous media. In aqueous solution, the hydrophobic regions of the polymer chains forms a hydrophobic core, while the hydrophilic ones are oriented outwards the aqueous medium, providing solubility and colloidal stability[71].

Depending on the nature of the polymer that is forming the core structure, molecules can be incorporated by physical, chemical and electrostatic interaction[73]. To ensure high loading capacity and controlled release profile for the incorporated molecule, core-forming block polymer must be chosen carefully to be in accordance with release pattern needed for its ultimate biological function. On the other hand, the hydrophilic corona is responsible for preventing non-specific absorption and dictates overall micelle hydrophobicity and charge, which ultimately effects biodistribution and pharmacokinetics[71].

Polymeric micelles-based delivery systems advantages include their small size, lower toxicity and longer blood circulation times. However, polymeric micelles are likely to dissociate, especially when using concentrations below the CMC. One way to prevent this event and maintain molecules inside the hydrophobic core, chemical crosslinking of micelles

can be done. However, crosslinked micelles may become too stable and may not release the total amount of drug required to achieve therapeutic efficacy[74].

2.3 Virus-Like Particles (VLPs)

Virus-Like-Particles (VLPs) are self-assembled nanoparticles derived from the proteins of viral capsids. Despite being composed of viral capsid proteins, VLPs are harmelss to human organism once they do not contain viral genomic material, making them non-infectious and non-replicative[75]. Yeasts and mammalian cells are the most frequently used in delivery systems. Examples comprises hepatitis B virus (HBV) and human papillomavirus (HPV) VLP-based vaccines[76]. This delivery system has been used to load a range of molecules, including nucleic acids, peptides and proteins through both covalent and noncovalent approaches[75].

Immunostimulatory molecules, like nucleic acids, can be loaded into VLPs to act as adjuvants and thus, activating the innate and adaptive immune systems. Also, VLPs can display several tumor antigens on its surface for targeting different cancers. Tumor self-antigens incorporated onto the surface of VLPs would be taken up, processed, and presented to T cells, eliciting potent anti-tumor immune responses[75,76]. Similar to other NPs, VLP stability, manufacturing cost and avoiding phagocyte-mediated clearance are still the major challenges[76].

2.4 Dendrimers

Dendrimers are globular macromolecule polymers, that can be distinguishable in three parts: i) a hydrophobic central core with two or more reactive groups, ii) repeated units covalently attached to the central core (branching dendrons) and iii) surface functional groups that define dendrimer surface hydrophobicity (Figure 5)[77].

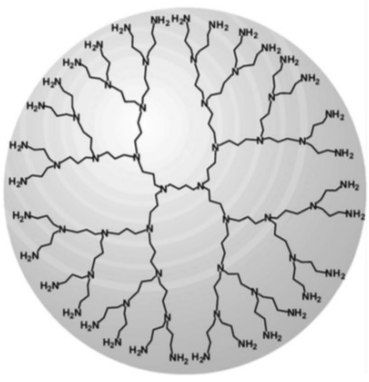

Figure 5 Structures of propylene imine (PPI) dendrimers. The alkyl chain and tertiary amines make PPI dendrimers non-polar. In acidic condition, dendrimers surface charge is cationic. TAAs and immune-modulators are encapsulated into the hydrophobic core, while targeting moieties are covalently conjugated to the dendrimer surface to interact with specific molecules expressed on targeted cell[78].

In ovarian adenocarcinoma, mAbs have been attached to the dendrimers's surface to selectively destroy tumor cells. Giving an example, mAbK1-poly (propylene imine) (PPI) dendrimer with entrapped Paclitaxel was capable of reducing tumor volume and prolong animal survival[79].

Moreover, their biocompatibility, bioavailability, multiple surface functionalization and excellent cellular and therapeutic cancer molecules uptake, makes dendrimers a promising platform for peptide and genetic delivery[77,78]. One interesting feature is dendrimers capacity of encapsulating or conjugating similar or different molecules[80].

However, some drawbacks can be pointed out. Dendrimers have strong binding affinity towards heavy metal ions, amphiphilic lipids, nucleic acids, among others. For instance, once administrated, dendrimers can complex with iron and thereafter, diminish the amount required for oxygen delivery and peroxide metabolism[78]. Similar to others nanocarriers, dendrimer surface charge determines the dendrimers' interaction with phagocytes. Cationic dendrimers with NH_2^- surface groups are reported to be more cytotoxic than anionic ($COOH^-$) and neutral ones, despite being more internalized. Negative and neutral surface charge are less recognized by the reticuloendothelial system (RES) and, thus, have higher systemic circulation time[78].

Due to dendrimers toxicological observations at molecular, cellular and tissue level, dendrimers are rapid cleared and have lower uptake by tumor cells. Consequently there is still a long way before dendrimers reach the market[77,78].

2.5 Inorganic nanocarriers

Besides gold nanoparticles (AuNPs) have shown good biocompatibility, size, shape and surface functionalization can be controlled, in contrast to other inorganic carriers such as silica NPs[81]. Other features include large surface:volume ratio, easy synthesis, and magnetic properties that allows nanocarrier tracking within the cells[77]. Due to all AuNPs characteristics mentioned above, AuNPs are being used in detection and diagnostics, biolabeling and drug delivery of peptides, proteins and nucleic acids[78].

Recently, several groups have observed that AuNPs can improve adjuvant delivery, with particular focus on CpG. CpG-AuNPs promote $CD4^+$ T cell and cytokine secretion, leading to improved $CD8^+$ T cells responses. Lee and colleagues (2014) observed that when bare gold NPs were injected into two *in vivo* tumor models, they reshaped the TME leading to inhibition of tumor growth and reduced tumor angiogenic factors[82].

Yet AuNPs shows some cellular cytotoxicity due to the vast available AuNPs size and shapes, which makes it difficult to predict cell type internalization mechanism[81].

2.6 Polymeric NPs

Polymeric NPs are promising vaccine delivery systems not only because they can be easily functionalized, but also due to their stability, entrapment and/or adsorbance capacity, surface area and ability to control the release of both hydrophilic and hydrophobic molecules. With all the features mentioned, NPs can be internalized, their content can be delivered to the APCs intracellular compartment and thus improving vaccine efficiency[83].

To achieve successful vaccination, the choice of polymers used for carrying TAAs is important. As the process of antigen cross-presentation to T cells is a fast and key step in cancer vaccination efficiency, the polymers constituting the NPs must be able of disrupting the endosomes in a restrict period of time to avoid antigen fully degradation[84]. The timing of tumor antigen release is crucial for an effective vaccine. If the antigen release kinetics is too slow, the amount of antigen available to be presented is reduced[85]. In this regard the polymers that compose NPs should be capable of releasing antigens in a fine-tuned and continuous manner to activate DCs and to ensure that an optimal concentration is maintained at the APCs. If all conditions are verified, T cell activation and memory antibody responses are expected[85].

Aliphatic polyesters, such as polylactic acid (PLA) and poly lactic-co-glycolic acid (PLGA) are polymeric materials approved by FDA for delivering bioactive macromolecules, (including peptides, protein and nuclei acids), preventing their premature release and so, can offer reduction of injections frequency[64]. Other important feature is their capacity to disrupt endosome membrane and release antigens and adjuvants in a sustained manner. Plus, these aliphatic polyesters-based NPs can also be functionalized to target APCs receptor-mediated phagocytosis. That being said, and because these polymeric NPs presents low toxicity and biocompatibility, these polymers are extensively used in cancer drug delivery system[19,64].

Combining antigens and adjuvants into PLA nanocarriers, have been demonstrated to induce strong cellular and humoral immune responses, culminating in antibody (e.g. IgG and IgA) and cytokine (e.g. IL-2 and IFN-γ) release[64]. Plus it has higher circulation half-life in plasma and can decrease multi-drug resistance (MDR), which characterizes many anticancer drugs[64,86].

However, PLA presents some drawbacks. For instance, PLA hydrophobic nature can elicit an inflammatory response from the tissues of living hosts. Blends of PLA with various synthetic and biopolymers have been prepared in an effort to enhance PLA properties. In this context, one strategy applied is blending it with poly(glycolic acid) (PGA) *via* copolymerized process (being PLGA its product) to increase hydrophilicity[87].

At physiological pH, PLGA particles present negative charge due to the pKa of its groups on the polymer chain. When these NPs are taken up by the APCs, the acidic pH from the endosomes and lysosomes induce the protonation of the acidic groups of PLGA polymer (Figure 6). The inversion of NPs surface charge, allows PLGA particles to interact with endo-lysosome membrane, which explains their capacity to escape from them leading to antigen cross-presentation and induction of a CTL response [84,88].

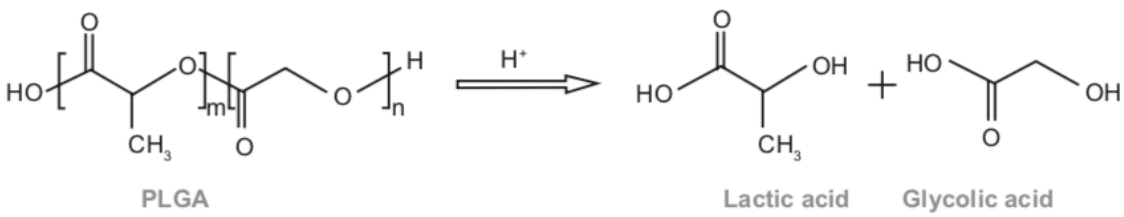

Figure 6 Degradation of polylactide-co-glycolide (PLGA) to lactic and glycolic acid(LA and GA)[1].

In the cytosol or at subcellular target compartments, the degradation and drug release process can be characterized in three stages: i) initial burst, ii) lag time and iii) fast release. In the first phase, upon *in vitro* administration, polymer channels are created inducing polymer degradation by non-enzymatic hydrolysis of the ester bonds, where a large amount of the entrapped molecules are released. After, the release rate decreases (lag time phase) either due to protein aggregation or incomplete release, depending on the interactions between the polymer and the drug[60]. This phase if followed by a faster release, which is the result of a local pH drop within the cytosol or at subcellular target compartments, that promotes polymer weight loss and drug release[89].

The degradation of aliphatic polyesters as PLGA occurs throughout polymer matrix equally (bulk-erosion) and not only on the surface of the nanocarrier. This is the result of water penetration in a faster extent rate than the erosion process (Figure 7)[90]. The resulting polymeric fragments from the NP matrix and surface (i.e. lactic and glycolic acids) are metabolized in the Krebs cycle and eliminated from the body as carbon dioxide and water[60].

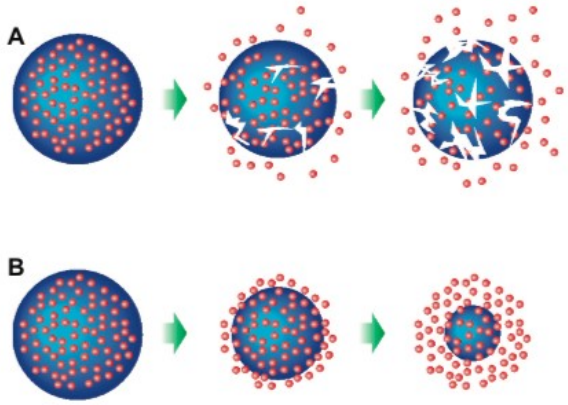

Figure 7 Degradation mechanisms of biodegradable polymeric drug carriers*:* A) bulk erosion, B) surface erosion[1].

Depending on the PLGA monomers ratio (PLA/PGA) (50:50, 65:35, 75:25 and 80:20) in the polymer chain, molecular weight, glass transition temperature (Tg) and hydrophobicity, the entrapped molecules release kinetics will be different. If lactic acid is in higher proportion than glycolic acid, the NP degradation will be slower as lactic acid is more hydrophobic and thus, absorbs less water. However, in the presence of 50:50 PLA/PGA ratio the degradation will be fastest as it has been shown to be completed in 50–60 days[60,91].

Yet *in vitro* NP degradation does not fully correlate with *in vivo* degradation, since it is not taking into consideration other parameters that influence polymer degradation, like enzymes. In this regard, designing a particle delivery system with a sustained release rate is a complex challenge[60,92].

3. Influence of NPs physicochemical properties in DCs uptake

3.1 NP functionalization

NP size can influence their interaction with the biological milieu including, molecules binding to NP surface, cell-NP binding, internalization and distribution in the intracellular compartments, vascular distribution, extravasation, and tissue diffusion. So, NP size influence the efficiency of peptide delivery[93].

To avoid RES recognition some researches are coating NP surface to make them more hydrophilic and to reduce the interactions between NPs and biomolecules present in blood lymph or interstitial fluid[94]. The usage of a PEG shell has been widely accepted to increase NPs systemic circulation time, which directly affects biodistribution and ultimately the therapeutic effect. Furthermore, coating NPs with hyperbranched PEG was reported to induce higher tumor uptake and cytotoxic PLGA NPs efficacy[13]. However due to long PEG chains, drugs and proteins can be difficult to encapsulate[22].

As said earlier, to ensure that NPs can be used as therapeutic alternative over radio and chemotherapy, the designed nanosystem must be capable of delivering both the selected antigen and adjuvant into APCs cytosol to be further presented to tumor cells and to elicit an immune response. In this sense, the interaction between APCs with the NPs is extremely recommended[22].

Generally, there are two ways to target the immune system, by taking advantage of the distinct pathophysiological features of tumor tissue (ie, passive targeting) or by actively targeting the drug carrier using target-specific ligands (ie, active targeting).

Passive targeting relies on the vaccine delivery system characteristics such as size, shape, surface charge and hydrophobicity/hydrophilicity that induce *per se* the rate and extent of internalization by APC, without any additional ligand[60]. An example of the passive target is the accumulation of NPs into the TME due to the enhanced permeability effect (EPR), where a deficient lymphatic drainage system and a leaky vasculature with greater tumor ECs pores are observed. Thereafter EPR effect favors NPs retention in tumors at a higher extent than in healthy areas[22].

On the other hand, the active targeting is based on NP surface functionalization with ligands towards different surface receptors on cells of the immune system, known to be involved in the recognition and internalization of pathogens[19].

As mentioned above, APCs possess a broad spectrum of cell surface receptors, including CLRs. The mannose receptor (MR/CD206), a member of family expressed on macrophages and DCs surface, is involved in the internalization of pathogens and endogenous glycoproteins through the recognition of sugars terminating in D-mannose, L-fucose or N-acetyl glucosamine[19,95].

According to Silva and colleagues (2014) functionalizing NPs with mannose, a natural polymannose isolated from the cell wall of *Saccharomyces cerevisae*, promoted higher cell-mediated and humoral immunity compared to non-functionalized NPs in a melanoma model. As so, NP functionalization with mannose can be used to improve APC targeting and provide direct intracellular access to immunotherapeutic molecules promoting potent immune responses[19,95].

3.2 Size

Particle size is one of most important factors affecting the endocytic mechanism and their intracellular biodistribution (endosomes/lysosomes, ER, Golgi complex and cytoplasm). However, the ideal dimensions of NPs for APC uptake are still under discussion[94].

As DCs can be found both in peripheral sites, such as epidermis and mucosa, and also in the LNs, different sizes may be considered for particulate systems.

Due to the diameters of the lymph vessels and the sinusoid in the spleen, only virus-sized particles ranging from 100 to 200 nm can travel directly through lymph system, reach the LNs and afterwards be internalized by LN-resident DC subsets ($CD8\alpha^{+}$)[2,19]. Concerning the DCs found in peripheral sites, nanosystems bigger than 200 nm will have to be internalized by peripheral iDC prior of reaching to LN, a process that takes approximately 24 hours[19].

The size of the NP also seems to influence their cellular uptake mechanism by the phagocytic cells (e.g macrophages, DCs) as well as biodistribution. More importantly, the induction of cytotoxicity by NPs are determined by its entry pathway and intracellular localization. Furthermore, intracellular trafficking and fate of NPs is a vital process to the success of NPs since NPs have to deliver specific biomolecules to sub-cellular compartment, which is an important step to obtain high therapeutic efficacy. Hence, understanding cellular uptake and intracellular trafficking of NPs is extremely important in designing safe and efficient therapeutic NPs[96].

NPs below 200 nm undergo clathrin-mediated endocytosis and particles between 50-80 nm internalize through the caveolae receptor. Both endocytic pathways can activate CTLs and Th1. Meanwhile, if the designed NP is larger than 0.5 μm, it will be submitted to macropinocytosis and phagocytosis by macrophages, inducing preferentially bacteria-like immune response with activation of Th2 cells and antibodies[2,19].

3.3. NPs morphology

It has become evident that size is not the only parameter that plays a significant role in dictating the fate of NPs within the body. NPs that present sphere morphology exhibit a larger surface area when compared to cylinders and cubical morphology. In this context, spherical-shaped NP dictates higher cellular uptake by APC[19,22].

3.4 NP surface charge

NPs surface charge also determines APCs uptake. As blood vessels and ECs membrane have negative charges due to the phosphorous group and other components, such as glycosaminoglycans and glycocalyx, it is expected that the cationic NPs induce phagocytic uptake at higher extent, when compared with negatively or neutrally charged ones[22,97]. Moreover after being internalized, cationic chitosan-based NPs can escape from lysosomes due to the "proton sponge" effect, where their unprotonated amines induce an influx of protons, chloride ions and water to the lysosome. The combination of osmotic swelling and repulsion between protonated amine groups leads to degradation of the lysosomal membrane and NP content release into the cytoplasm[98,99].

Although the surface charge of cationic NPs seems to be an advantage for cellular uptake even being nonspecific, some major drawbacks can be enumerated. These include rapid clearance, which translates to shorter blood circulation half-life and hence**,** compromises the delivery of the NP content. Also, due to the electrostatic interaction with negatively charged blood and serum proteins, cationic NPs can aggregate, which can cause greater toxicity compared to anionic and neutral NPs[94,100].

It has been described that NPs containing a slightly negative charge were able to accumulate efficiently within H-22 mouse liver cancer tumors *in vivo*. Upon NP uptake, it was

verified that macrophages could perform their phagocytic function independently of NPs charge[64,97].

Once all NP physicochemical properties were taken into consideration to guarantee the APCs uptake success, the cells are transported to LNs through the lymphatic system, where CTL and Th1 function will be activated and a specific and long-lasting immune response will be triggered (Figure 8).

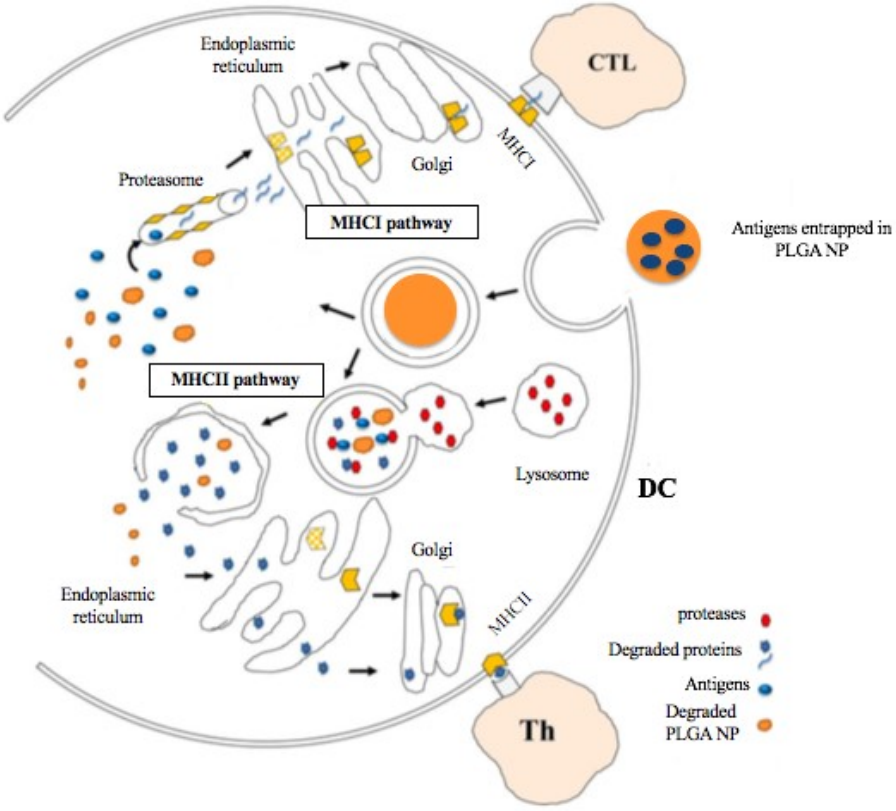

Figure 8 Schematic presentation of the intracellular trafficking of antigens entrapped into PLGA NP in DC. PLGA particles are taken up by endocytosis following binding to DC membrane. Antigens delivered by PLGA NP undergo 2 distinct intracellular pathways. From the phagosome to the cytosol pathway of cross-presentation, PLGA particles escape from the endosome, degrade in the cytoplasm, releasing the loaded protein gradually, which is further processed and complexed to the MHC class I molecules. Alternatively, the degradation of antigen loaded PLGA particle happens inside the endosome due to its acidic pH. The antigenic peptides are released, processed, being further presented via MHC class II pathway. CTL: T cytotoxic lymphocyte; Th: T-helper lymphocyte. Adapted from[60].

3.5 Administration route

Finally, NP size can also influence the administration route. Since tissues have not the same structure, transport kinetics and the delivery efficiency depends highly on the subsets of APCs

found at the site of injection and the route of administration[93,101]. Moreover, to effectively promote a potent immune response, the administration route should consider all the steps involved in the adaptive immune response, including antigen uptake and APCs activation, to activate naive T cells in an antigen-specific manner[102].

Common routes of administration of NPs include mucosal administration and parenteral administration: subcutaneous (s.c), intradermal (i.d), intramuscular, each with corresponding applications and unique features[93]. Mucosal administration of NPs can be accomplished via pulmonary, vaginal, intranasal, or even oral administrations[93]. Depending of the selected route of administration, different cells can internalize PLGA NPs. In a study conducted by Hamdy *et al.* (2011), it was shown a correlation between PLGA NPs internalized by DCs by s.c or i.d, while intraperitoneal injection (i.p) administration resulted in PLGA uptake by macrophages[60].

Antigens injected into the skin taken up by skin-resident DCs (LCs present in the epidermis and dermal DC) are transported from the periphery to lymphoid organs. In addition, phagocytic monocytes present in the systemic circulation can also take up antigens in the skin, differentiate into DCs and migrate to the dLNs. So targeting skin DCs can promote anti-tumor immune responses[103].

In addition, administering NPs into mucosal surfaces can elicit both mucosal and systemic immune responses, as it was shown when using pluronic-stabilized polyphenylene sulfide (PPS). These NPs reached the epithelium, translocate to either the circulation or lymphatics, leading to antigen-specific antibodies and cellular immune responses[93,104].

Several groups have shown that intracerebrally injected DCs migrate through olfactory nerves to nasal mucosa, where they would drain into cervical LN and activate T cells. These DCs can also induce the activation and migration of T cells found in the systemic circulation, to the brain[49]. Likewise, it has been found $CD4^+$ and $CD8^+$ T cells within the glioma tissue as well as macrophages (90%)[49].

4. Polymeric NP formulation method

To make sure that the selected preparation method is the most adequate to prepare NPs with the desired size and properties, which is the result of a complex equilibrium between the chemical components of the polymers and the formulation conditions, the nature of antigen, adjuvant and polymer employed and drug release profile should be considered[93,105].

Depending on the formulation method, nanospheres or nanocapsules can be synthetized (Figure 9) and the antigens and adjuvants peptides can either be entrapped in a liquid core surrounded by a polymer shell, dispersed or dissolved into the particle matrix and/or adsorbed on the nanoparticle surface[106].

Given the fact that the antigen adsorption is based on charged and hydrophilic interactions, it is expected that the adsorbed antigens onto NP surface will dissociate rapidly. Regarding antigen entrapment, antigens can be released upon uptake and polymer degradation inside of APCs. Additionally, entrapped antigens are more protected from degradation during the delivery and thus higher levels of antigens entrapped in NPs are internalized by APCs[2,107].

To develop the intended polymeric NPs, water/oil/water double emulsion solvent evaporation method has been extensively used for the entrapment of highly water soluble compounds, as well as hydrophobic molecules. Entrapment of peptides, proteins and nucleic acids prevents their degradation and enhances their loading efficiency. Moreover this method offers the possibility to entrap several molecules simultaneously and to enable the controlled release of those molecules[108,109].

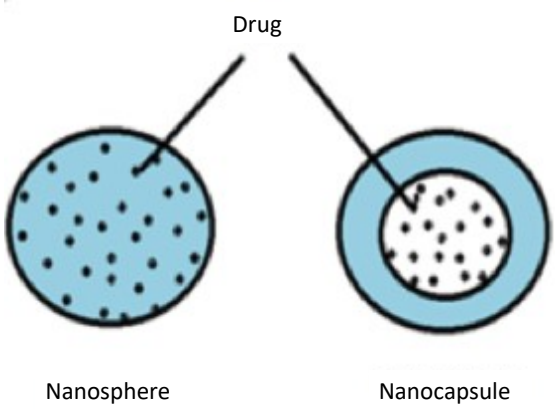

Figure 9 Difference between nanosphere and nanocapsule. Nanospheres are matrix spherical systems that have the therapeutic molecule homogenously dispersed into the particle matrix, whereas nanocapsules are vesicular systems, where the drug is surrounded by a polymer wall[106].

In this method, an aqueous solution composed by a hydrophilic surfactant (internal aqueous phase, w_1) is emulsified in a solution of a polymer previously dissolved in organic solvent. The resulting primary emulsion (w_1/o) is then dispersed in a second aqueous phase (external aqueous phase, w_2) containing another stabilizer to form double emulsion ($w_1/o/w_2$). Then the double emulsion created is added to a larger aqueous phase and stirred for one hour for solvent evaporation (Figure 10)[110].

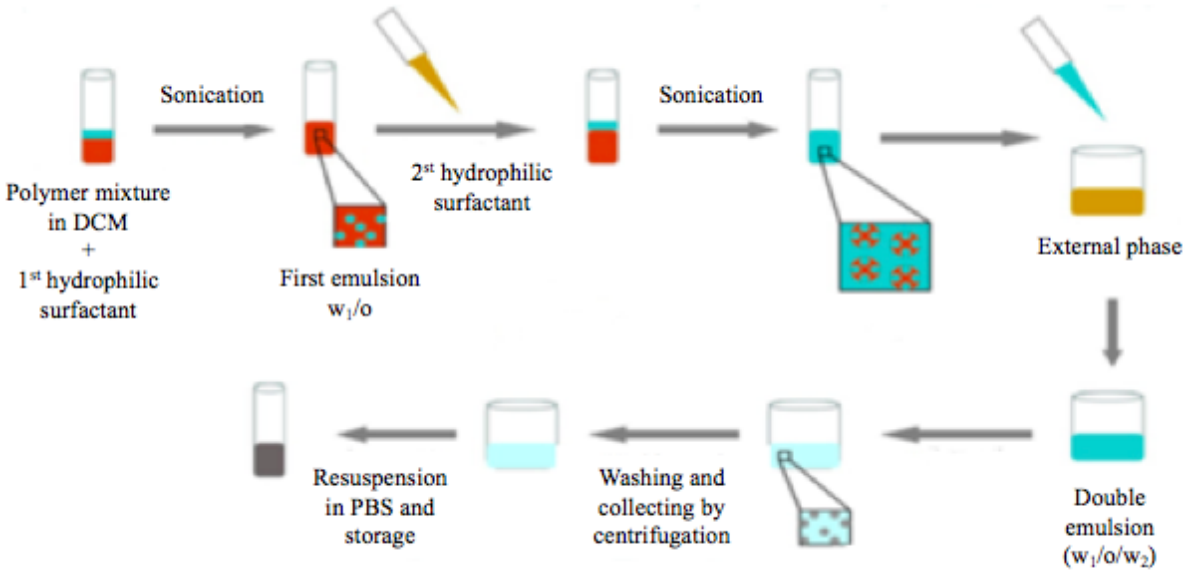

Figure 10 Schematic representation of the double emulsion evaporation method[111].

4.1 Role of surfactants in NPs characteristics

The choice of the surfactants is a crucial parameter to insure the emulsion stability and droplet size. During the production of NPs two different non-ionic emulsifiers are combined. Non-ionic surfactants have more advantages than the charged ones because: i) have better capacity to solubilize poorly water-soluble molecules, ii) have high biocompatibility and iii) can modulate MDR that has been shown to impact drug pharmacokinetics. Moreover colloidal stability, cell uptake and cytotoxicity are strongly influenced by NPs composition, including surfactants[112,113]. Here, we will focus our attention into poly(vinyl alcohol) (PVA) and vitamin E d-α-tocopheryl polyethylene glycol 1000 succinate (TPGS) surfactants and their effect on

the formation of small particles with uniform size distribution, as well as impact on the overall immune-mediated impact on DCs[114].

PVA is a surfactant used to lower the surface tension between the organic and the aqueous phases, two immiscible phases, thus reducing their miscibility and dispersion. In general, increasing PVA concentration, the particle size decreases due to the formation of more stable droplets, decreasing both the size and the polydispersity. All features mentioned above, make PVA a strong w/o internal emulsion stabilizer[115–117].

Other surfactant used in the formulation of NPs delivery systems is TPGS that acts as a steric stabilizer of $w_1/o/w_2$ emulsions. Other features includes biocompatibility and the capacity for both hydrophilic and hydrophobic molecules to be entrapped[114]**.** It has been used as a surfactant in PLGA, PLA-TPGS and PLGA-PEG NPs, since it has high entrapment efficiency (EE) and increases NPs diffusion through different biological membranes, like skin, cornea and intestinal walls[118,119]. When compared to PVA alone and in combination with TPGS, PLGA-PVA/TPGS NPs exhibited high emulsification efficiency in terms of EE, decreased polydispersity index (PdI) as well as burst release of NPs[120].

Besides this surfactant has been revolutionizing cancer therapy since it can act as an anticancer molecule, promoting different apoptosis signalling pathways through both caspase-dependent and caspase-independent DNA damage and disruption of mitochondria membrane, which results in the depletion of intracellular ATP and ROS release[119]. The reduced ATP level can inhibit the activity of P-gp, also known as multidrug ATP-binding cassette sub-family B member 1 (ABCB1) and ultimately inhibit the efflux pump and decrease drug accumulation in cells[119]. Therefore, the use of TPGS as a surfactant can modulate MDR. Moreover, Yang *et al.* (2018) studied the effect of TPGS in both tumorigenic cells and non-tumorigenic cells in breast cancer cells and concluded that TPGS only has a selective cytotoxic affect in the tumorigenic cells[119].

All these factors culminate in cancer cell specific destruction, once TPGS does not trigger any apoptosis event in normal cells and tissues. Ideally, it can be combined with conventional therapies to increase treatment efficiency[119].

As mentioned along this work, to trigger anti-glioma and anti-metastatic melanoma lymphocyte responses, the immune system must be able to have access to tumor antigens. Several studies suggest that the presentation of brain antigens to APCs happens outside of the CNS, in the cervical lymph nodes present in the back of the neck. As nasal cavity is a doorway between systemic circulation and CNS, some researchers are using poloxamers to ensure the mucoadhesion of NPs and to facilitate its spreading on the mucosa[49].

Poloxamer are a non-toxic and non-ionic synthetic triblock copolymer constituted by hydrophilic poly (ethylene oxide) (PEO) and hydrophobic poly (propylene oxide) (PPO) with a PEO-PPO-PEO structure[121].

Depending on EO/PO ratios, Pluronic can present different molecular mass and different hydrophilic-lipophilic balance (HLB). HLB traduces the relation between the hydrophilic and the lipophilic portion of the non-ionic surfactant. High values cause destabilization of the internal droplets, while low values may lead to instability between oil globules[112].

Within poloxamers, Pluronic F127 (PF-127) is the most biocompatible polymer. Here we use PF-127 with HBL values between 18 and 23, which can solubilize higher amounts of water-soluble molecules[122,123].

Similar to the previously described surfactants, Pluronic is widely used in drug delivery since it can lower oil–water interfacial tension and increase the viscosity of the continuous phase, contributing to the formation of stable emulsions with long-term stability. Additionally, it is approved for oral and intravenous administration due to their low toxicity, solubilizing capability, biocompatibility and high drug loading[72,124]. When its concentration is below the critical micelle concentration (CMC), copolymer can also increase the efficiency of multiple anticancer agents against various drug resistant cancer cells by affecting diverse cellular functions, compromising ATP synthesis, drug efflux transporters molecules, apoptotic signaling pathways, mitochondrial respiration and gene expression[86]. Furthermore, this non-ionic amphiphilic poloxamer can be adsorbed into NPs surface (*via* PPO chains) to inhibit particle aggregation in the colloidal system prolonging *in vivo* circulation time. The presence of Pluronic in NPs composition also showed to facilitate the release of entrapped proteins protecting them from the acidic medium along PLGA NPs degradation[86,125].

Chapter 2 – Objectives

The specific goals of this research project were to:

1. Develop a stable and non-toxic biodegradable polylactic-based NP delivery system.

2. Investigate the impact of non-mannosylated PLGA-PEG, PLA/PLGA-PEG and PLA/PLGA NPs, as well as mannosylated PLA/PLGA-PEG and PLA/PLGA NPs properties on DCs internalization.

3. Develop NPs entrapping combinations of mlmp3D81N glioblastoma or MUT30 metastatic melanoma neo-antigens, with CpG and Poly (I:C) as adjuvants, aiming at the DC activation and further induction of a strong and long-lasting immune response towards brain malignant cells.

4. Understand how different surfactants impact DCs internalization and the activation markers on migratory and resident DCs at dLNs

.

Chapter 3 – Materials and methods

3.1 Materials

Poly(lactic-co-glycolic acid) (PLGA) Resomer® RG 502 (lactide: glycolide 50:50) with an average molecular weight (Mw) = 17 kDa was purchased from Evonik (Darmstadt, Germany). Poly(lactic-co-glycolic acid) (PLGA) conjugated with polyethylene glycol (PEG), i.e. PLGA-PEG with an average Mw= 20kDa, Poly(vinyl alcohol) (PVA) with an average MW = 13–23 kDa), D-α-Tocopherol polyethylene glycol 1000 succinate (TPGS), Pluronic F127 (PF-127) with an average of 12.6 kDa, Dichloromethane (DCM), Trypan blue solution 0.4% liquid, sterile-filtered and suitable for cell culture, fluorescamine, Trinton X-100 and phosphate buffered saline (PBS), were purchased from Sigma-Aldrich (St. Louis, MO, USA). Polylactide (PLA) with an average Mw = 2000Da was purchased from PolySciences , Inc (UK). Mannose-grafted poly(lactic-co-glycolic acid) (PLGA) (man-PLGA) and mannose-grafted PLGA-PEG (man-PLGA-PEG) were synthesized by a "click" chemistry reaction established in our group[126]. CpG ODN 1826 (TCCATGACGTTCCTGACGTT) (costume made) was purchased from Microsynth (Balgach, Switzerland). Double distilled water was used after filtration in a Millipore® (Millipore, Billerica, MA). Polyinosinic:polycytidylic acid (PolyI:C) (HMW) VacciGrade (Cat.# Vac-pic) was purchased from InvivoGen (San Diego, CA, USA). 3-[4,5-dimethylthiazol-2-yl]-3,5 diphenyl tetrazolium bromide (MTT) (Cat# 0793-1G) was purchased from AMRESCO® (Solon, OH, USA). Ovalbumin (OVA, average MW=45kDa). Minimum Essential Medium α (MEM- α) was purchased from Thermofisher, Dimethyl sulfoxide (DMSO) was purchased from Merck (Darmstadt, Germany). Propidium iodide (PI) solution at 1 mg/mL was purchased from invitrogen Fetal bovine serum (FBS), were purchased from Gibco. Murine GM-CSF cat#315-03-20UG were purchased from PeproTech, inc. Ethylenediamine tetracetic acid (Trypsin-EDTA) solution and Penicillin/Streptomycin (Pen-Strep) were purchased from Life Technologies (Carlsbad, CA, USA). Granulocyte-macrophage colony stimulating factor (GM-CSF) and interleukine-4 (IL-4) were purchased from PeproTech Inc. (Rocky Hill, NJ, USA). Fixation/Permeabilization Kit (BD Cytofix/CytopermTM Cat: 554,714) was purchased from BD Bioscience, San Diego, CA, USA. Glioblastoma neo-antigen mLmp3D81N (AALLNKYA) and melanoma neo-antigen MUT30 (PSKPSFQEFVDWENVSPELNSTDQPFL) were purchased to GeneCust Europe.

3.2 Methods

3.2.1 Synthesis of nanoparticles

NPs were designed considering the optimal physicochemical properties that NP should have to improve their activity, taking in consideration the literature of recent years[64,94]. Properties including size, surface charge, structure and hydrophobicity are fundamental in this process.

Polymeric NPs were prepared by the double emulsion ($w_1/o/w_2$) solvent evaporation method. The single emulsion (o/w) was formed by adding 10% (m/v) PVA into an organic phase, composed by the polymer dissolved in DCM on ice, using a ultrasonics sonifier processor (Brandson digital sonifier) for 15s at 20%. A 2.5% (m/v) TPGS solution was added to the o/w primary emulsion and a second sonication was performed under the previously described conditions. The double emulsion was added dropwise to an external aqueous phase composed by 0.25% (m/v) PVA or 0.125% (m/v) PF-127 aqueous solution. Solvent evaporation was carried by magnetic stirring during 1 h, thus enabling the formation of NPs. The polymeric NPs were harvested by centrifugation at 22,000g for 45 min, 4°C (BECKMAN GPR centrifuge), washed twice to remove the excess of surfactant and finally re-suspended in PBS pH 7.4. NPs were kept at 4°C before any further experiment.

Different NPs were developed using a mixture of two aliphatic polyesters, PLGA and PLA, looking at the DC passive targeting and mannose-grafted NP to target CD206 receptor at APC surface. NPs for passive targeting included PLGA-PEG, PLA/PLGA-PEG (80:20 $w_1/o/w_2$) and PLA/PLGA (80:20 $w_1/o/w_2$), whereas functionalized NPs were composed by PLA/PLGA-Mannose (80:20 $w_1/o/w_2$) or PLA/PLGA-PEG-Mannose (80:20 $w_1/o/w_2$) (Figure 11). The polymer ratio in the formulation has been previously optimized in our laboratory in terms of physicochemical properties[127].

Differences in nanoparticle matrix and the surfactant used are summarized in table 1.

Table 1- Composition of the distinct NP formulations

Nanoparticle matrix	IP[1]	EP[2]	FP[3]
PLGA-PEG	10% (m/v) PVA	2.5% (m/v) TPGS	0.25% (m/v) PVA
PLA/PLGA-PEG			
PLA/PLGA-PEG-Mannose			
PLA/PLGA			0.125%PF-127
PLA/PLGA-Mannose			0.25%PVA
PLA/PLGA-Mannose			0.125%PF-127

[1]IP- internal phase, [2]EP- external phase, [3]FP, final phase

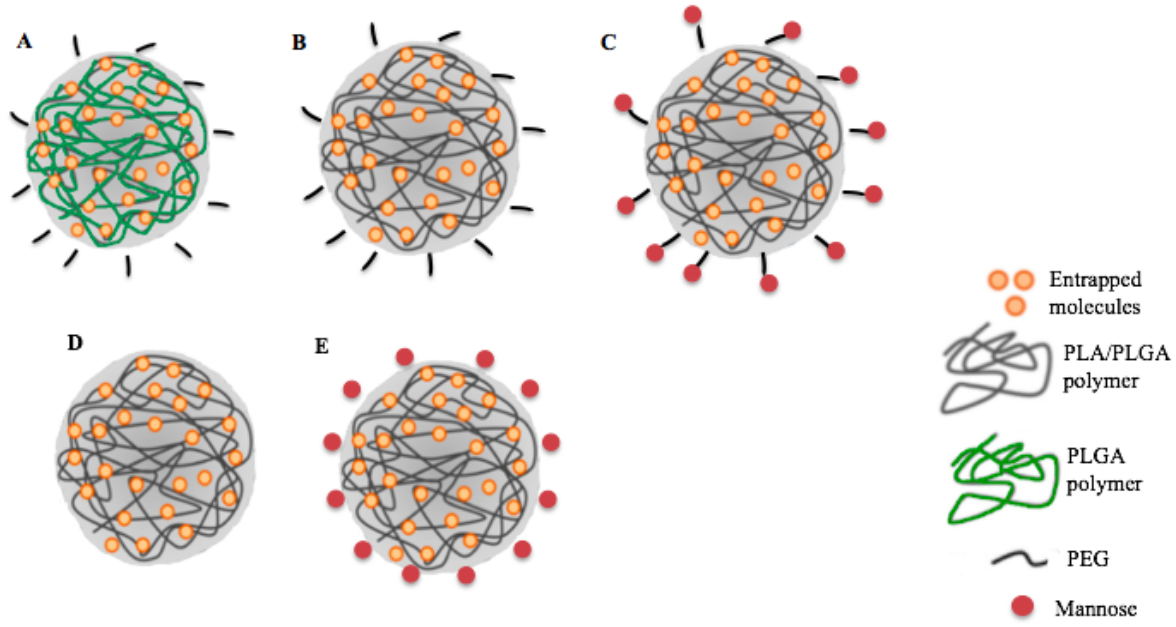

Figure 11 Schematic representation of the different intended NPs. A. PLGA-PEG NP B. PLA/PLGA-PEG NP C. PLA/PLGA-PEG-Mannose NP D. PLA/PLGA NP E. PLA/PLGA-Mannose NP.

3.2.2 NP physicochemical properties characterization

NPs were diluted to a final concentration of 0.2 mg/mL and NP mean size and polydispersity index (PdI) were determined by Dynamic Light Scattering (DLS) using Malvern Nano S (Malvern Instruments, UK) at 25°C). NP surface charge in H_20 and KCl was inferred from the determination of ζ-potential that was assessed by Laser Doppler Velocimetry (LDV) with Malvern Nano Z (Malvern Instruments, UK). Measurements were analyzed in triplicate.

NP morphology was investigated by tapping mode atomic force microscopy (AFM) (Nanoscope IIIa Mulimode AFM, Digital Instruments, Veeco), using silicon tips (ca. 300 kHz) at a scan rate of ca. 1.6 Hz. Samples were diluted in purified water (10 mg/mL) and a drop was placed onto mica and dried overnight. Prior to the analysis, the samples were submitted to N_2. NP morphology was analyzed at room temperature.

3.2.3 NP stability

Polymeric NPs were dispersed in PBS pH 7.4 and kept at 37 ºC and 4 ºC. In an attempt to mimic *in vivo* NP degradation profile, NPs were also dispersed in PBS pH 5.7 and storage at 37 ºC. Over 7 weeks, the average size and surface charge of 0.2 mg/mL NP suspensions were measured by DLS and LDV.

3.2.4 Cell line culture conditions

Murine immature dendritic cells (JAWSII cell line) were cultured in minimum Essential Medium Eagle - alpha modification (α-MEM) containing 10% (v/v) of fetal bovine serum (FBS), 1% (v/v) Penicillin/Streptomycin (Pen-Strep), 1% (v/v) sodium pyruvate and 100 μg/mL of granulocyte-macrophage colony stimulating factor (GM-CSF).

3.2.5 Evaluation of NP cytotoxicity in murine immature DC line

In vitro NP cytotoxicity was evaluated using the 3-[4,5-dimethylthiazol-2-yl]-3,5 diphenyl tetrazolium bromide (MTT) assay. This assay depends on the cellular reductive capacity to metabolize the MTT to a highly colored insoluble formazan product. Briefly, JAW SII DCs

were plated at a density of 25 x 10^3 cells/well in 96-well plates containing α-MEM medium and GM-CSF. After overnight incubation at 37°C, the medium was removed and new medium, which contained the NPs suspension was added into the wells ($N = 3$) in 96-well plates. Three different concentrations of NPs were used: i) 0.25 mg/mL; ii) 0.5 mg/mL; iii) 1 mg/mL. After 96 h of incubation in a humidified 37°C, 5% CO_2 incubator, the cell viability was evaluated using the MTT colorimetric assay. For the assay, 10 mg/mL MTT stock solution was incubated into each well. After 4 h of incubation, 100 µL of dimethyl sulfoxide (DMSO) was added to dissolve the formazan crystals. Absorbance was then analyzed at 570 nm using a microplate reader (Bioteck Instruments ELx800). The cells in culture medium were used as negative control, while the positive control was obtained after cell treatment with 10% (v/v) Triton X-100 to give relative cell viability.

NPs cytotoxicity was also evaluated with propidium iodide (PI) to study cellular nucleus integrity. Briefly, JAW SII DCs were plated at a density of 25 x 10^3 cells/well in 96-well plates containing α-MEM medium and GM-CSF. After 4 h of incubation at 37° C, 5% CO_2 incubator, the medium was removed and new medium containing the NP suspension at 0.5 mg/mL was incubated with the cells for different time points (2, 5, 18, 24, 48, 72, and 96 h). After 96 h, the cell viability was evaluated using fluorescence PI. For the assay, 200 mL of FACs buffer containing 2 µg/mL of PI were incubated into each well. The cells in culture medium were used as a negative control, while the positive control was obtained after cell treatment with PI to give relative cell viability.

3.2.6 NP internalization

To verify if the produced NPs could be internalized by APCs, NPs were developed using 5 mg/mL PLGA-Cy5 After 2, 5, 18, 24, 48, 72 and 96 h of incubation with immature JAWSII cell line, the plates were centrifuged at 1300 rpm, 4 ºC for 5 min. PBS was added on ice and cells were centrifuged (5 min, 1000 rpm, 25 ºC). Cells were re-suspended on ice and FACS buffer (PBS sterile buffer + 2% (v/v) FBS) was added in each well. A minimum of 25 x 10^3 cells per sample were analyzed by LRS II Fortessa flow cytometer (BD Bioscience).

3.2.7 Determination of antigen loading

Antigens were added in the internal phase with 10% (m/v) PVA and plain NPs, only with 10% (m/v) PVA in the internal phase, served as control. The supernatants obtained from NP centrifugations and washings were collected to quantify the entrapment efficiency (EE %, Eq. (1)) and the loading capacity (LC μg/ml, Eq. (2)) of the entrapped antigens. Collected supernatants were submitted to successive 1:2 dilutions in a 96-plate wells and fluorescamine (3 mg/mL, DMSO) was added to the plate for 15 min protected from light. The relative fluorescence units (RFU) were measured at 360 nm excitation and 465 nm emission wavelengths, using a microplate reader (POLARstar OPTIMA, BMG Labetech Durham, NY, USA).

EE is defined according to the following equation:

$$EE\% = \frac{Wload}{Wtotal} x\ 100\% \qquad \text{(Equation 1),}$$

LC is defined as drug-to-carrier ratio according to the following equation:

$$LC = \frac{Wload}{Wcarrier} \qquad \text{(Equation 2),}$$

where, W_{load} is the amount of peptide actually loaded in the NPs, W_{total} the total amount of peptide added for NP preparation and $W_{carrier}$ is the amount of polymer that carries drug/peptide.

3.3 Animals

Female C57BL/6J mice (16 weeks old) was purchased from ICG (Oeiras, Lisboa, Portugal) and housed in the animal facility of the Faculty of Pharmacy at University of Lisbon. All animal procedures were completed with Faculty of Pharmacy, University of Lisbon guidelines. Protocols were reviewed and approved by Portuguese competent authority for animal protection, Direcção Geral de Alimentação e Veterinária, Lisbon, Portugal and performed in accordance with NH guidelines.

3.3.1 Impact of nanovaccines on APC activation and maturation in vivo

C57BL/6J mice female (n = 3/group) 16-week-old was injected by subcutaneous (s.c.) hock immunization with fluorescent 0.75 mg of PLGA-Cy5 labeled NPs suspension. C57BL/6J mice female were randomized into one of the groups presented in the table 2. The groups immunized with PBS and the combination of antigen and immune adjuvant in solution were used as controls (table 2). After 17 h post-immunization, inguinal LNs were harvested and homogenized in a single cell suspension. To understand the internalization level of the NPs by distinct myeloid cell populations, the percentage of $CD11c^{+}$MHCII cells (classical DCs), $CD11b^{+}CD11c^{-}$ (macrophages), $CD11b^{+}$ $CD11c^{+}$ (migratory DCs) and $CD11b^{-}$ $CD11c^{+}$ (LN resident DCs), the cells were stained with fluorescent-labeled anti-mouse antibodies against CD11c, MHCII (I-Ab), MHCI (H-2Kb), CD80 and CD86 and CD40, for 20 min protected from light. Samples were acquired with a LSR Fortessa X-20 flow cytometer (BD Bioscience) and analyzed with FlowJo software (Treestar, San Carlos, CA).

Table 2- Polymeric NPs composition as nanovaccines against brain tumors.

Group	Nanoparticle matrix	Antigen	Adjuvants
1	PBS		
2		mlmp3 D81N	Poly (I:C) + CpG
3		MUT30	
4	PLA/PLGA- Mannose	mlmp3 D81N	
5	PLA/PLGA	MUT30	
6	PLA/PLGA-Mannose	MUT30	
7	PLA/PLGA-PEG-Mannose	MUT30	

Statistical analysis:

Differences in mean values of the results were evaluated by one-way analysis of variance, ANOVA, followed by Tukey's multiple comparison test. The values are expressed as mean ± standard deviation (SD). The statistical analysis was performed using GraphPad Prism 8 from GraphPad Software (San Diego, USA).

Chapter 4 - Results

4.1 Formulation and characterization of empty NPs

Different NPs with distinct chemical compositions were developed and optimized. All NPs produced contained 10% (v/v) PVA and 2.5% (v/v) TPGS as internal and external phase, respectively. Final aqueous phase contained 0.25% (v/v) PVA. Depending on the NP composition, Z-average, PdI and zeta-potential presented different values as shown below (Table 3).

Table 3- Physicochemical characterization of polymeric NPs (Z-average, PdI and zeta-potential). Values are presented as mean ± SD of three individual batches.

Nanoparticle matrix	Z-Average (nm)	PdI	Zeta-potential (mV)
PLGA-PEG	188.62 ± 2.11	0.13 ± 0.02	-29.56 ± 1.73
PLA/PLGA-PEG	172.59 ± 0.43	0.09 ± 0.01	-25.48 ± 0.92
PLA/PLGA-PEG-Mannose	182.17 ± 2.27	0.16 ± 0.01	-16.27 ± 0.42

NPs displayed a size range between 172.6 ± 0.43 nm and 186 ± 2.08 nm, and a narrow particle size distribution (PdI ranging from 0.09 ± 0.01 to 0.16 ± 0.01), indicating a homogenous NP population. At pH 7.4, NPs presented a zeta potential ranging from -29.56 ± 1.73 to -16.27 ± 0.42 mV.

AFM was used to further characterize size, shape and surface morphology of the NPs. A drop of each NP suspension was placed onto freshly cleaved mica and dried with N_2 prior to examination. Both PLGA-PEG and PLGA-PEG-Mannose NPs presented slightly rough surface and spherical topography (Figure 13 & 14).

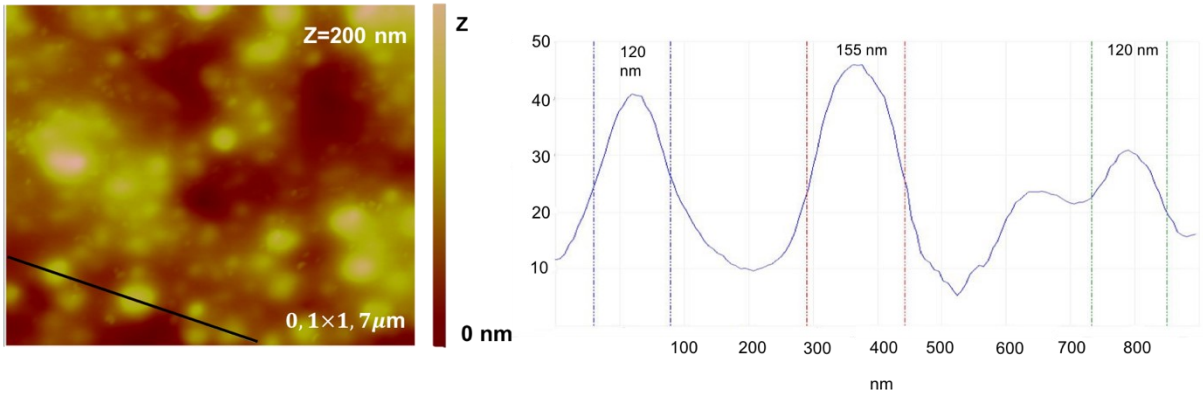

Figure 12 AFM analysis of PLGA-PEG NP size and morphology.

The high content of hydrophilic PEG chains at the NP surface tends to adsorb water molecules, which makes it hard to see NP boundaries. AFM images reveled a small NP size (< 155nm) and low diameter distribution.

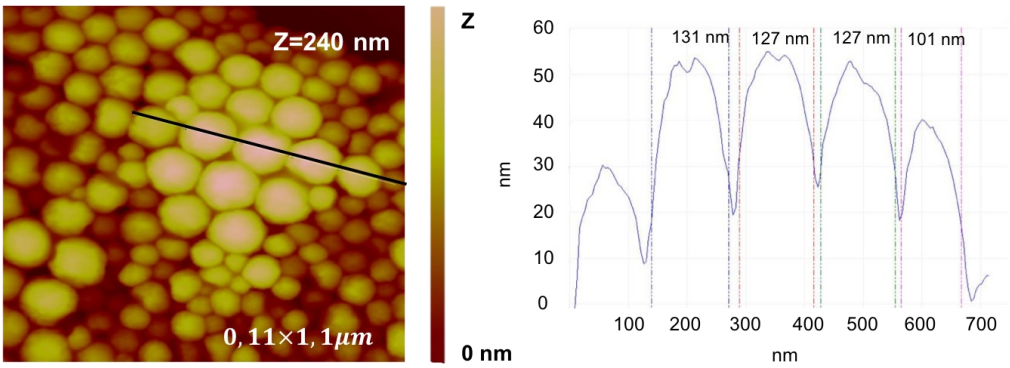

Figure 13 AFM analysis of PLA/PLGA-PEG NP size and morphology

Comparing to PLGA-PEG, AFM image of PLA/PLGA-PEG NP show a more disperse population comprising NPs with different sizes (75-131 nm) (Figure 13). Again, the presented images exhibit smaller NP size when compared to the DLS results.

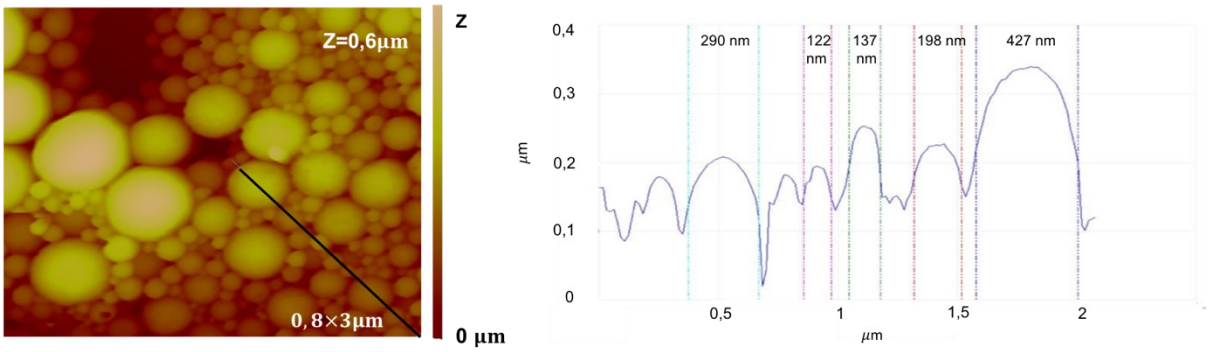

Figure 14 AFM analysis of PLA-PLGA-PEG-Mannose NP size and morphology

Among the NPs produced, PLA/PLGA-PEG-Mannose demonstrated a wider particle size distribution (122-427 nm), as well as larger diameters (Figure 14). Similar to the previous NPs, the AFM image reveals a spherical surface for these carriers.

4.2 Evaluation of NP stability

NP average size and zeta-potential were measured over 7 weeks, when dispersed in PBS pH 7.4 and stored at 37°C and 4°C.

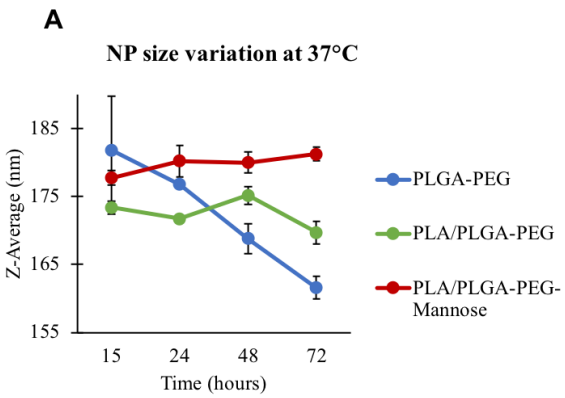

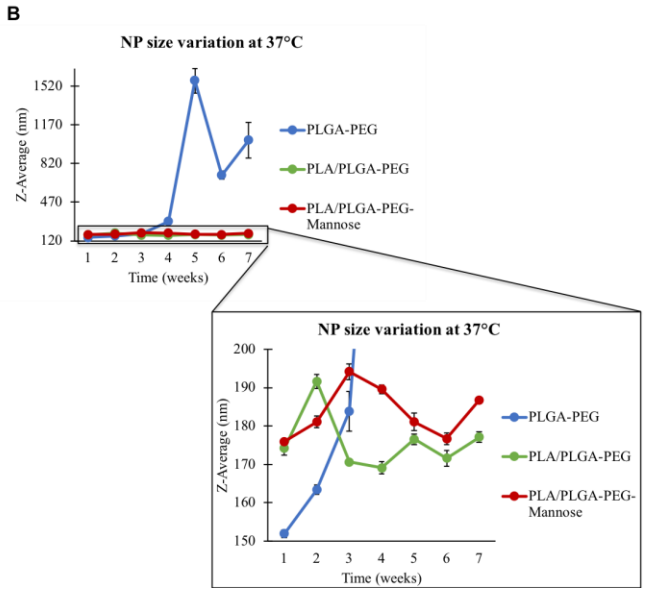

Figure 15 Representation of NP size variation over 7 weeks: A. in the first 72 h and B. over seven weeks. All NPs were stored at 37 ºC in PBS pH 7.4. Values are presented as mean ± SD, N=1, n=3.

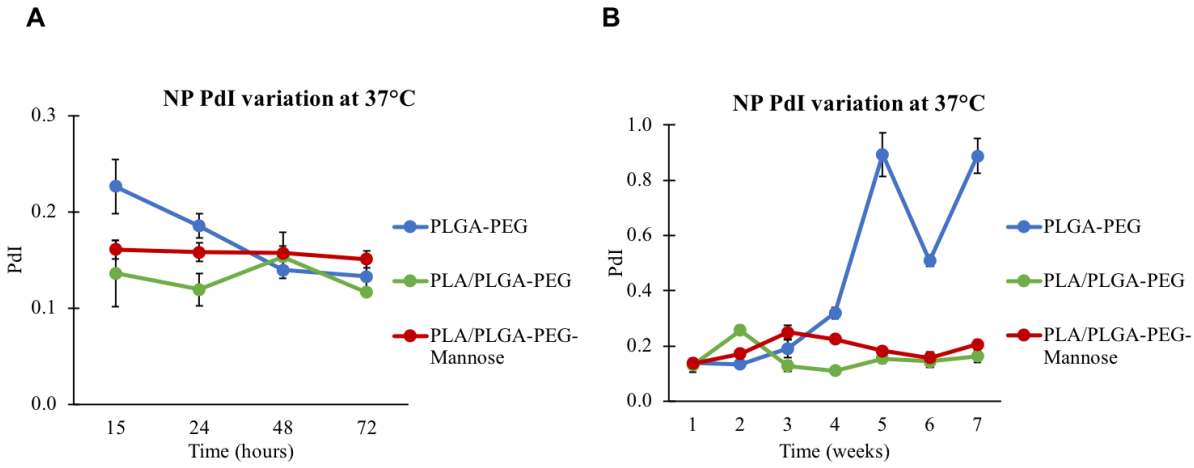

Figure 16 Representation of NP polydispersity index (PdI) variation over 7 weeks: A. until 72 h and B in weeks. All NPs were stored at 37 ºC in PBS pH 7.4. Values are presented as mean ± SD, N=1, n=3.

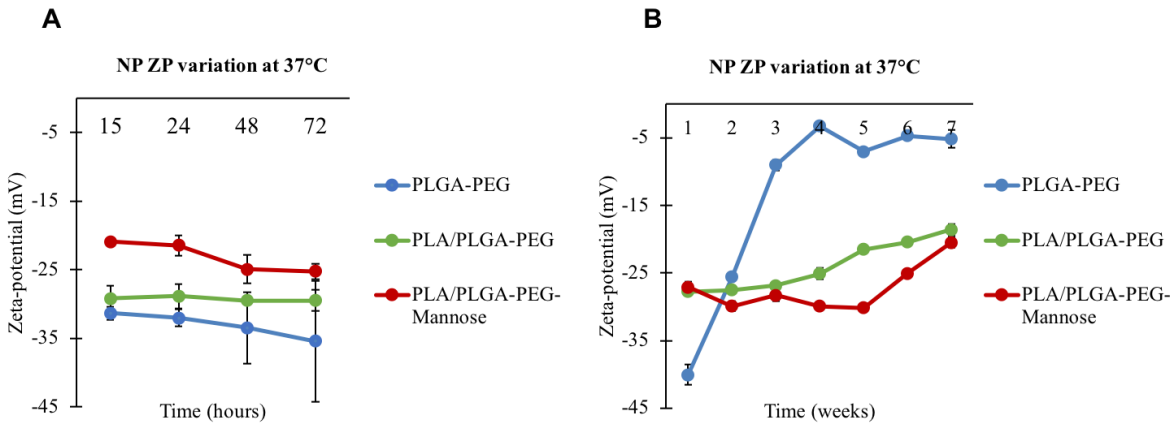

Figure 17 Representation of NP zeta-potential (ZP) variation over 7 weeks: A. until 72 h and B in weeks. All NPs were stored at 37 ºC in PBS pH 7.4. Values are presented as mean ± SD, N=1, n=3.

In the first 72 hours of the stability study at 37°C, the hydrodynamic diameter of the PLGA-PEG NP decreased from 181.8 ± 8 nm to 161.5 ± 1.7 nm, as well as the PdI to values lower than 0.2 (Figures 15 & 16). From the 3rd to the 4th week, there was an increase on NP size, but the major size difference occurred in the 5th week, when the size reached 1569 ± 112.7 nm. Along with size, the PdI also increased to 1 (Figures 15 & 16). Regarding the PLA/PLGA-PEG and the PLA/PLGA-PEG-Mannose NPs, NPs average size remained with no significant changes until the first week ~174.6 ± 1.4 nm and 179.8 ± 1.5 nm, respectively. With the exception of week 3rd and 4th, the PdI of PLA/PLGA-PEG-Mannose NP remained stable ~ 0.18 ± 0.01 and higher than the one obtained for the PLA/PLGA-PEG NP (~0.15 ± 0.01) (Figure 16).

Looking into graphic B of the NP size variation (Figure 15), the size of the PLA/PLGA-PEG and PLA/PLGA-PEG-Mannose NPs remained with no significant changes ~175.8 ± 1.5 nm and ~182.2 ± 1.4 nm, respectively. Comparing the PdI, the PLA/PLGA-PEG-Mannose NP showed higher values (~ 0.20 ± 0.01) compared to the 0.15 ± 0.01 obtained for PLA/PLGA-PEG NP (Figure 16). Nevertheless, both NPs presented smaller size and PdI than PLGA-PEG NP.

Regarding NP surface charge, the zeta-potential of PLGA-PEG NP decreased from -31.3 ± 0.7 mV to -40.1 ± 1.5 mV by the end of 1st week. But from week one, the zeta-potential increased abruptly until -3.3 ± 0.3 mV on the fourth week. From that time point, zeta-potential stabilizes at –5.6 ± 0.8 mV (Figure 17). Concerning the PLA/PLGA-PEG NP, the zeta-potential did not show significant changes in the first 72 h of study, presenting an average of -29.3 6 ±

0.9 mV. From 1st week, the zeta-potential slightly increased until -18.6 ± 0.8 mV. On the other hand, from the first 15 h, the surface charge of PLA/PLGA-PEG-Mannose NP stabilized in 30.1 ± 0.6 mV on the 5th week. After that point, the zeta-potential became less negative (-20.5 ± 0.7 mV) (Figure 17).

In general, the zeta-potential of all NPs became less negative, with PLGA NPs presenting the most positively charged surface and PLA/PLGA-PEG-Mannose NP the most negative one.

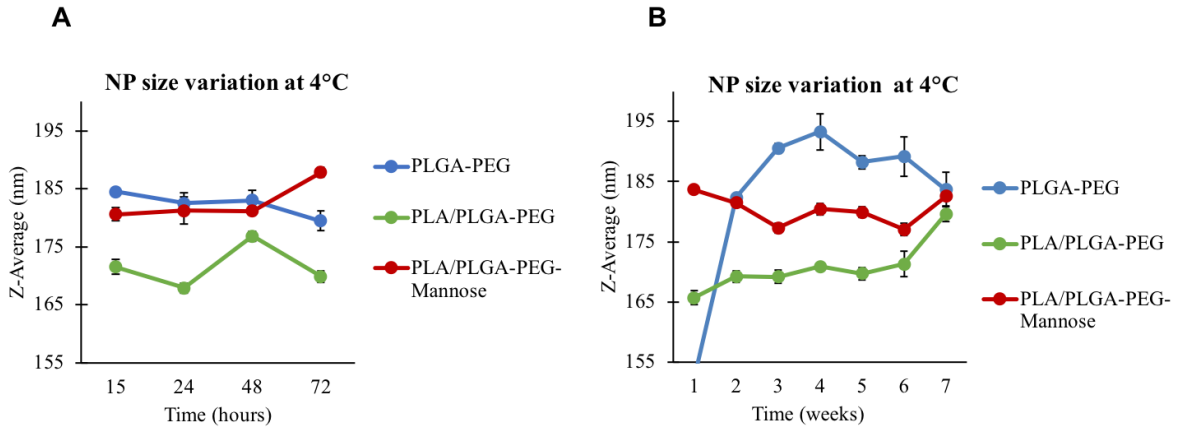

Figure 18 Representation of NP size variation over 7 weeks: A. until 72 h and B in weeks. All NPs were storage at 4 ºC in PBS pH 7.4. Values are presented as mean ± SD, N=1, n=3.

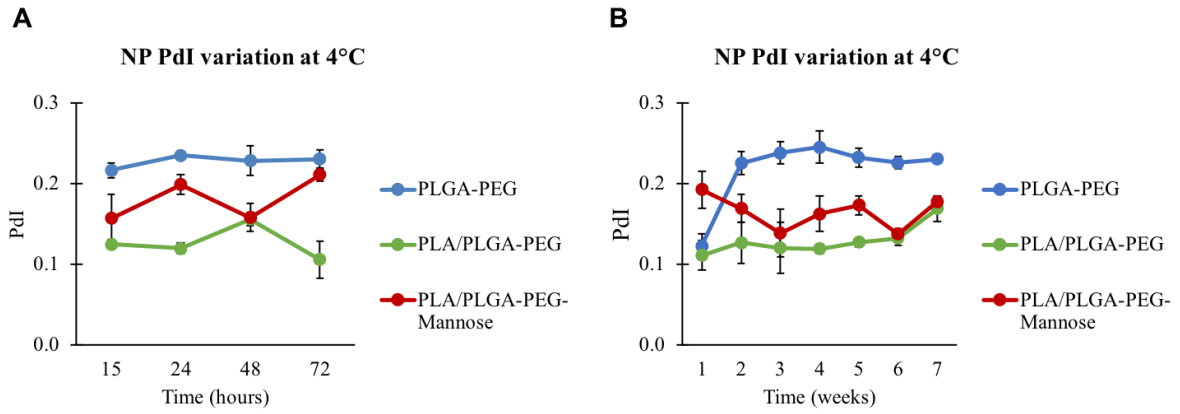

Figure 19 Representation of NP polydispersity index (PdI) variation over 7 weeks. A. until 72 h and B. in weeks. All NPs were stored at 4 ºC in PBS pH 7.4. Values are presented as mean ± SD, N=1, n=3.

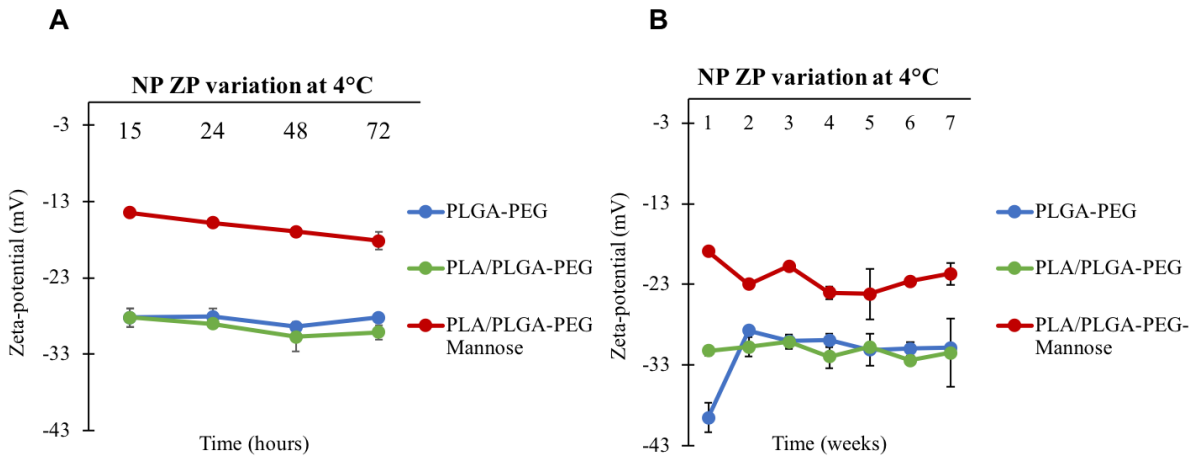

Figure 20 Representation of NP zeta-potential (ZP) variation over 7 weeks: A. until 72 h and B in weeks. All NPs were stored at 4 ºC in PBS pH 7.4. Values are presented as mean ± SD, N=1, n=3.

In the first hours of the stability study at 4 ºC, the variation of PLGA-PEG NP size was not significant (Figure 18). However, size continuous to increase reaching ~193.2 ± 3.0 nm until the fourth week. From that point, NPs size slightly decreased and the PdI remained stable (~ 0.22 ± 0.01) (Figure 19). Comparing PLA/PLGA-PEG with PLA/PLGA-PEG-Mannose NPs, both presented similar average sizes (~ 171.6 ± 1.0 nm and ~ 182.7 ± 1.3 nm, respectively). Both NPs remained stable until the 7th week with no significant size changes (Figure 18). The same pattern was verified for the PdI, where PLA/PLGA-PEG NP showed slightly higher PdI values (0.17 ± 0.01 and 0.13 ± 0.01, respectively) (Figure 19). Overall, the PLGA-PEG NP and PLA/PLGA-PEG-Mannose NP showed similar hydrodynamic diameters (182.7 ± 1.6 nm and 181.2 ± 0.9 nm, respectively) and PLA/PLGA-PEG NP exhibited slightly smaller size with 171.1 ± 1.1 nm (Figure 18).

Surface charge of all NPs remained stable with no significant changes over time (Figure 20). PLGA-PEG and PLA/PLGA-PEG NPs presented similar surface charge by the end of the 7th week, having the PLA/PLGA-PEG-Mannose NP the least negative surface charge.

4.3 NPs degradation profile

The aim of this study was to develop a nanoparticulate delivery system to target APCs, and to deliver antigens to cytoplasm (for MHC I presentation) and to the endosome pathway (for MHC II presentation). For that, the designed NPs must be capable of release the antigens. As the lysosomal pH level is approximately 5, all NPs were submitted to acidic pH to predict NPs degradation profile *in vivo*.

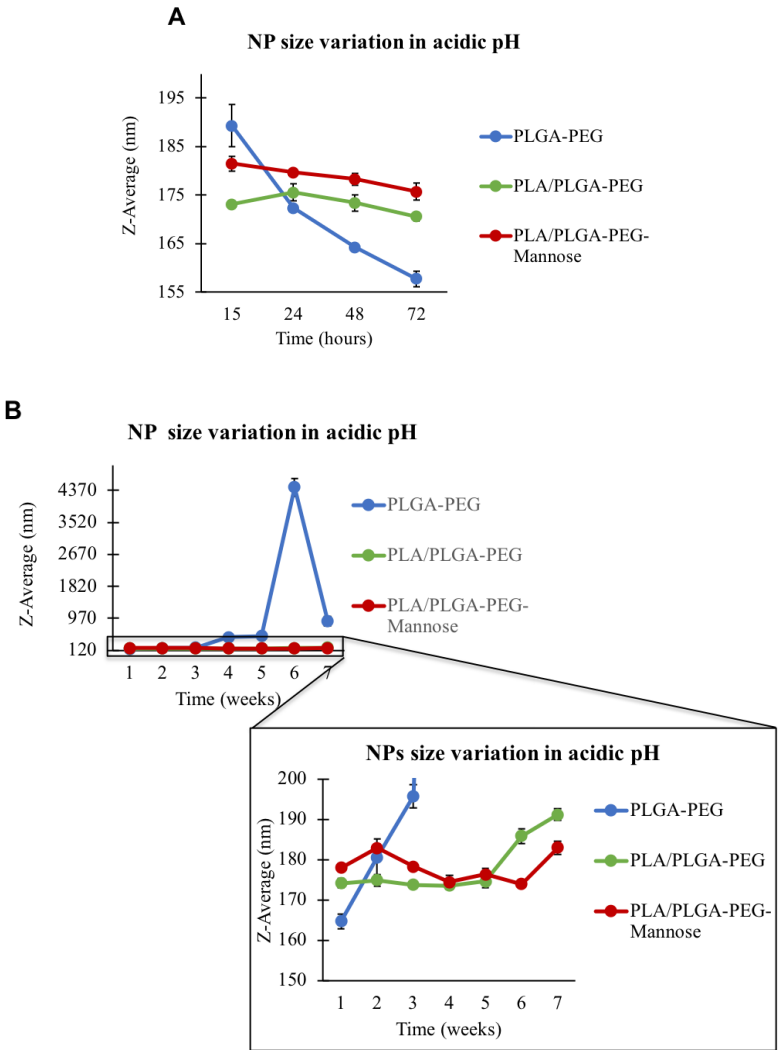

Figure 21 Representation of NP size variation over 7 weeks: A. in the first 72 h and B. over seven weeks. All NPs were stored at 37 ºC in PBS pH 5.7. Values are presented as mean ± SD, N=1, n=3.

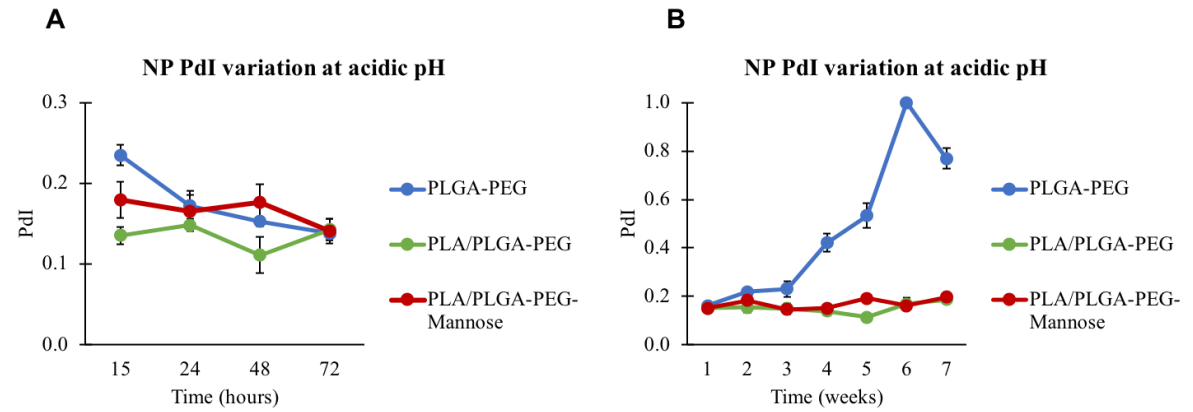

Figure 22 Representation of NP polydispersity index (PdI) variation over 7 weeks. A. until 72 h, B. in weeks. All NPs were stored at 37 ºC in PBS pH 5.7. Values are presented as mean ± SD, N=1, n=3.

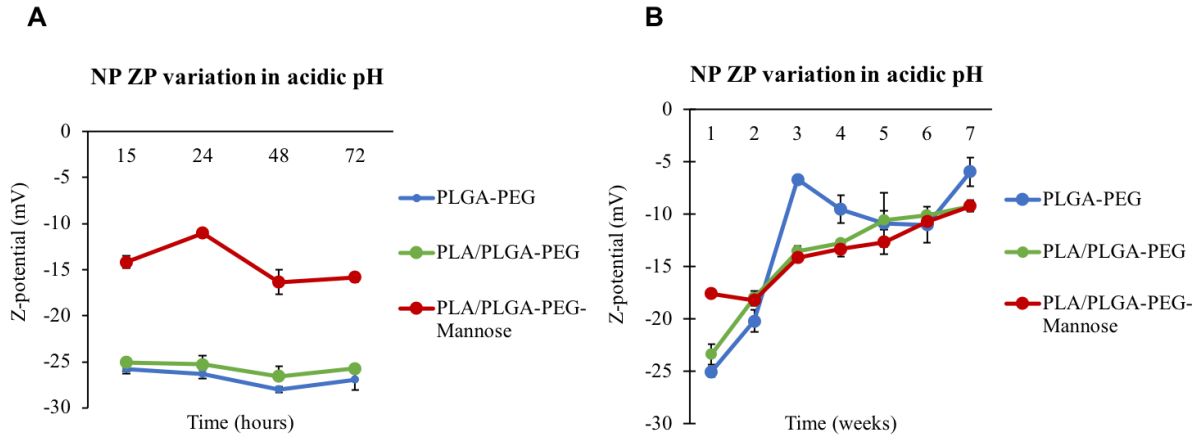

Figure 23 Representation of NP zeta-potential (ZP) variation over 7 weeks. A. until 72 h, B. in weeks. All NPs were stored at 37ºC in PBS pH 5.7. Values are presented as mean ± SD, N=1, n=3.

In the first hours, the hydrodynamic diameter of PLGA-PEG NP decreased from 189.3 ± 4.3 nm to 164.7 ± 1.8 nm. From the 2nd week, however, NP size increased to values higher than 275 nm, being the highest value of 4449 ± 233 nm obtained at the 6th week. The PdI also abruptly increased (Figures 21 & 22).

Until the 5th week, the size of PLA/PLGA-PEG and PLA/PLGA-PEG-Mannose NPs remained stable with no significant changes in their hydrodynamic diameter (~173.8 ± 1.21 nm and ~178.5 ± 1.6 nm, respectively). From the 6th week the NP size of PLA/PLGA-PEG NP size increased to 191.2 ± 1.5 nm whereas the size of PLA/PLGA-PEG-Mannose NP remained with no significant changes (Figure 21). Yet, both NPs showed smaller size, while comparing

with PLGA-PEG NP (892.9 ± 118.32 nm). The PdI of PLA/PLGA-PEG NP remained unaltered until the 5th week (~ 0.14 ± 0.01) and increased to 0.19 ± 0.01 at the 7th week. The PdI values of PLA/PLGA-PEG-Mannose NPs followed the same trend, transited from 0.16 ± 0.02 to 0.2 ± 0.01. In addition, the PdI of both NPs was lower than the one presented by PLGA-PEG NP (0.37 ± 0.02).

According to Figure 23, in the first 72 h of the study, all produced NPs presented a zeta-potential with no significant changes, being the PLGA-PEG NP the most negative one with -26.8 ± 0.6 mV. On the other hand, the PLA/PLGA-PEG-Mannose NP exhibited the least negative charge (-14.4 ± 0.6 mV). After that period, the zeta-potential of all NPs became more positive, with PLGA-PEG NP showing marked variation in the surface charge (-20.2 ± 1.0 mV to -6.7 ± 0.4 mV). At the 7th week, both PLA/PLGA-PEG and PLA/PLGA-PEG-Mannose NPs presented similar surface charge (-9.2 ± 0.3 mV and -9.2 ± 0.5 mV, respectively).

4.4 *In vitro* cytotoxic assays

In order to verify if the produced NPs could affect the viability of DCs, JAWSII cells were submitted to MTT assay following their incubation with each NP formulations, and the cell viability was assessed.

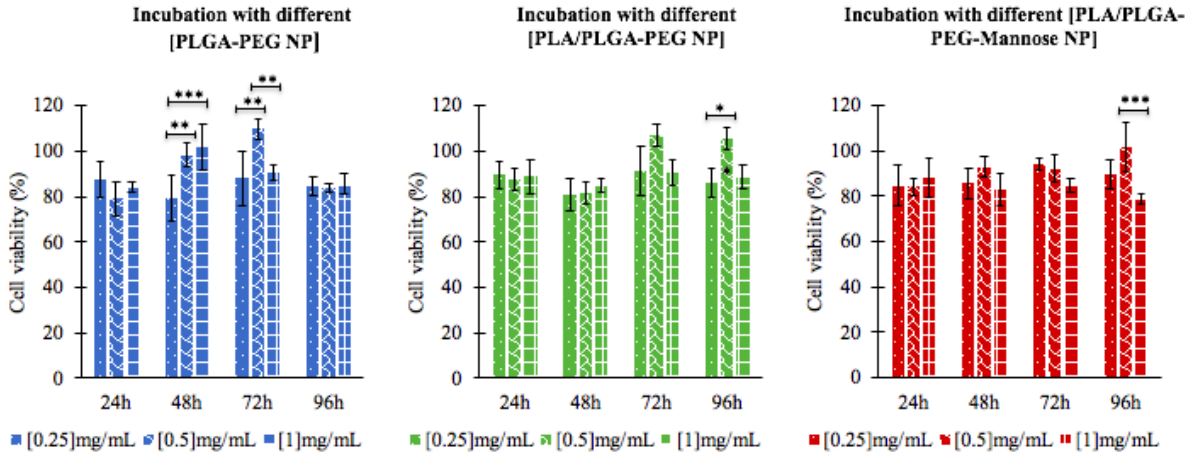

Figure 24 NPs are not cytotoxic against JAWSII cells. A. PLGA-PEG NP, B. PLA/PLGA-PEG NP, C. PLA/PLGA-PEG-Mannose NP at different time points. Results were obtained by MTT assay and the percentage of viable cells in each well was calculated as the absorbance ratio between nanoparticle-treated and untreated control cells. Culture medium and Triton X-100 were used as negative and positive controls, respectively. Results were shown as the average cell viability of triplicate wells. Data are presented as mean + SD, $N = 3$ n = 3. Two-way ANOVA followed by Tukey post-hoc test were used to compare PLGA-PEG PLA/PLGA-PEG and PLA/PLGA-PEG-Mannose NPs concentration could be cytotoxic to JAWSII cell line. *$p < 0.05$, ** $p < 0.01$ and *** $p < 0.001$

Regardless of NP concentration, the cell viability of immature DCs cells was not affected by the NPs, presenting cell viabilities higher than 80%. The cytotoxicity of the NPs was also inferred through apoptosis studies performed with NPs at 0.5 mg/mL, by flow cytometry.

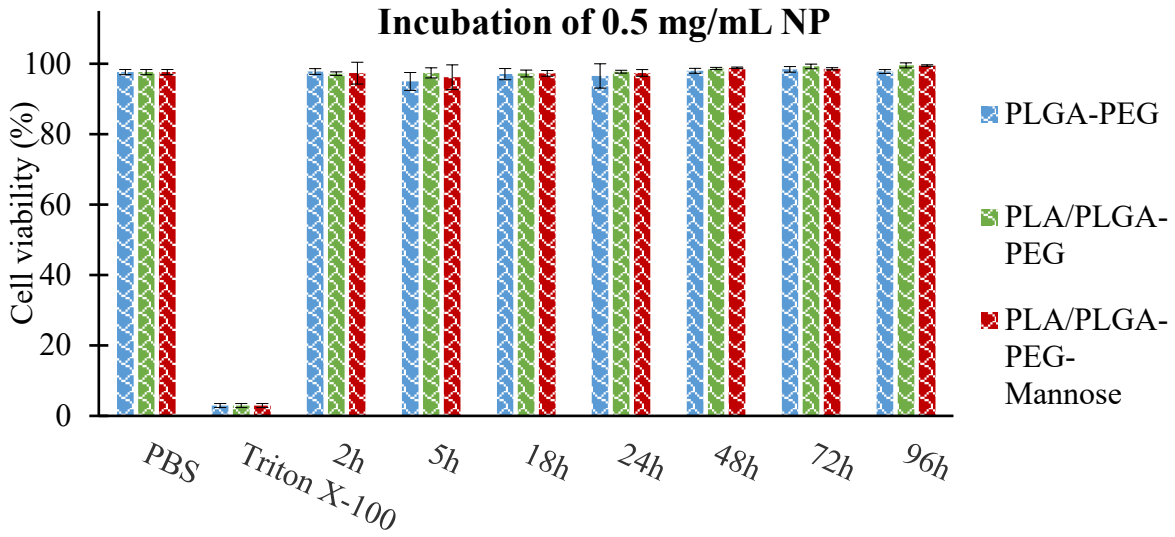

Figure 25 Cell viability of JAWSII cells by flow cytometry. NPs were incubated at different time points. The percentage of viable cells in each well was calculated as the absorbance ratio between nanoparticle-treated and untreated control cells. Cells were labelled with propidium iodide (PI). Data are presented as mean + SD, $N = 3$, n = 3.

With NPs at 0.5 mg/mL, none of the NP formulations led to a reduction in cell viability for the period of time studied (2-96 h), once cell viability was higher than 90%.

4.5 Cellular uptake kinetics

NP internalization by DCs is a critical step for the induction of an effective immune response. NP internalization profile was determined by flow cytometry and therefore, NPs were labeled with 5 mg/mL PLGA-Cy5 and incubated in JAWSII cells for 96 h at 37 ºC.

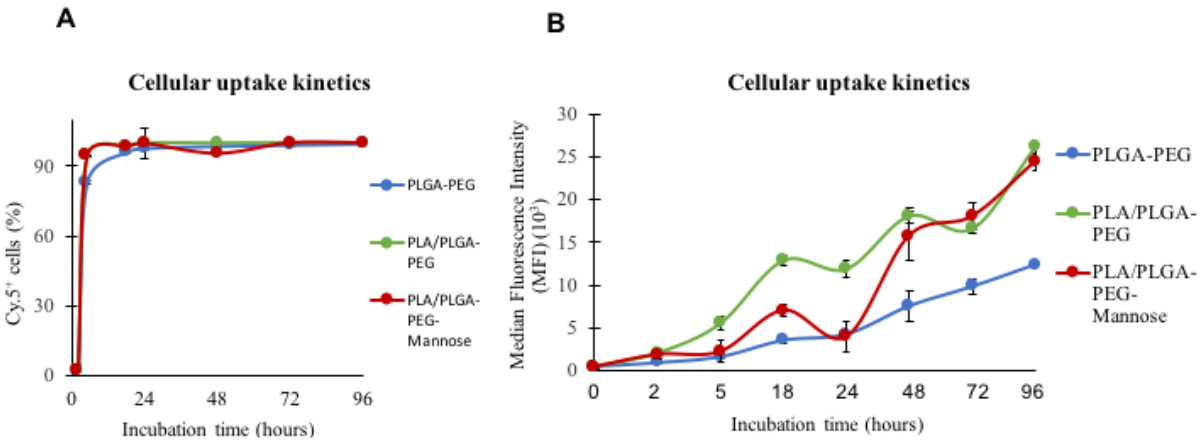

Figure 26 Extensive *in vitro* PLA NP internalization by JAWSII. Flow cytometry analysis was performed to detect Cy5-labeled NPs in JAWS II after 2, 5, 18, 24, 48, 72 and 96 h incubation *in vitro*. A) Percentage of $Cy5^+$positive cells in the population and B) Median fluorescence intensity (MFI) of NPs internalization. Data are presented as mean + SD, $N = 1$, $n = 3$.

Overall, the internalization levels increased with the incubation time. JAWSII cell lines internalized all the produced NPs. PLA/PLGA-PEG and PLA/PLGA-PEG-Mannose NPs presented higher internalization by murine immature DCs, compared to PLGA-PEG NP. Independently of the NP composition, the *in vitro* results demonstrate that the internalization rate is higher after 96 h of NP incubation.

4.6 Determination of antigen and adjuvant loadings

So far, three different NPs systems have been characterized with the aim of co-encapsulating antigens and adjuvants, to induce a specific and long-term immune response. Along the presented work, PLA/PLGA-PEG-Mannose NP exhibited distinguishes physicochemical properties that make this PLA-based NP (PLA/PLGA-PEG and PLA/PLGA-PEG-Mannose) a promising delivery system, when compared to PLGA-PEG NP. With this, the entrapment efficiency (EE) (%) and loading capacity (LC) (µg/mg) were assessed using OVA antigen model only in PLA/PLGA-PEG-Mannose NP. This NP revealed high EE (93.21% ± 4.52) and was possible to load 46.6 (± 2.26) µg of OVA antigen per mg of NP. These results obtained by fluorescamine assay, indicate that this NP can entrap antigens at an amount suitable for further *in vivo* assays.

Particulate-based system for brain tumors

Analyzing all the data collected so far, PLGA-PEG NP did not show advantage in DC internalization. With these PLA-based NPs, namely the PLA/PLGA, PLA/PLGA-Mannose and PLA/PLGA-PEG-Mannose NPs were used for study activation and subsequent maturation of APC, namely DCs. Since PLA can trigger adaptive immune responses (humoral and cellular) and also local immune responses after nasal administration[64], these PLA-based NPs will be further explored as a platform to deliver combinations of antigens and TLR ligands against melanoma brain metastases and glioblastoma (Table 4). With different combination of polymers within PLA/PLGA, PLA/PLGA-Mannose and PLA/PLGA-PEG-Mannose NP matrix, we intend to study how the use of a spacer, as PEG at the surface of NP will impact DC activation and maturation, looking at the induction of a strong but specific immune response against brain tumors.

As mentioned before, PF-127 has a great dispersion capacity that enhance the mucus penetration[128]. With this characteristic, it promotes NP delivery into the systemic circulation and to LN in the back of the neck to further present tumor antigens. After this process, we expected that the activated T cells would bypass the BBB to kill tumor cells. However, the exact mechanisms of drug delivery for nose-to-brain is not well understood[44,49]. Based on this, besides PVA we will also test PF-127 in the final formulation phase and study the impact on DC activation and maturation. Accordingly, NPs contained 10% (m/v) PVA, 2.5% (m/v) TPGS as internal and external surfactants, respectively, and 0.25% (m/v) PVA and 0.125% (m/v) PF-127 were tested in final phase (Table 4).

Table 4- Representation of nanovaccines composition (polymer matrix, neo-antigens and adjuvants) for brain tumors.

	Melanoma nanovaccines			**Glioblastoma nanovaccine**
Surface	PLA-PLGA	PLA/PLGA-Mannose	PLA/PLGA-PEG-Mannose	PLA/PLGA-Mannose
Entrapped	MUT30 and CpG + Poly (I:C)	MUT30 and CpG + Poly (I:C)	MUT30 and CpG + Poly (I:C)	Mlmp3 D8N1and CpG + Poly (I:C)
FP[1]	0.125% PF-127	0.25% PVA	0.25% PVA	0.125% PF-127

[1]FP- final phase

Depending on the NP composition, Z-average, PdI and zeta-potential presented different values as shown in table 5.

Table 5- NPs physicochemical characterization (z-average, PdI and zeta-potential) of polymeric PLA NP. Results are presented as mean ± SD of N=1, n=3.

Nanoparticle matrix	FP[1]	Size[2] (nm ± SD[3])	PdI[4] ± SD	Zeta-potential (mV ± SD)
Plain PLA/PLGA	0.125% PF-127	214 ± 2.9	0.18 ± 0.01	-3.84 ± 0.81
MUT30-PLA/PLGA	0.125%PF-127	236 ± 33	0.21 ± 0.03	-4.21 ± 0.83
Plain PLA/PLGA-Mannose	0.25%PVA	188 ± 1.8	0.13 ± 0.02	-3.29 ± 0.34
MUT30-PLA/PLGA-Mannose	0.25%PVA	235 ± 4.7	0.22 ± 0.01	-3.43 ± 0.20
PlainPLA-20% PLGA-PEG-Mannose	0.25%PVA	191 ± 3.2	0.14 ± 0.01	-1.59 ± 0.12
MUT30-PLA/PLGA-PEG-Mannose	0.25%PVA	216 ± 2	0.20 ± 0.02	-1.88 ± 0.24
Plain PLA/PLGA-Mannose	0.125%PF-127	188 ± 1.8	0.13 ± 0.01	-14.5 ± 0.53
Mlmp3 D81N-PLA/PLGA-Mannose	0.125%PF-127	186 ± 12.1	0.13 ± 0.03	-12.3 ± 0.27

[1]Final phase, [2]Z-average hydrodynamic diameter, [3]Standard deviation, [4]Polydispersity index

NPs displayed a size range between 186 ± 12 nm and 236 ± 33 nm and a narrow particle size distribution (PdI ranging from 0.13 ± 0.01 to 0.22 ± 0.1), indicating a homogenous NP population. At pH 7.4, NPs presented a zeta potential ranging from -14.5 ± 0.53 to -1.59 ± 0.12 mV.

Table 6- Entrapment efficiency (EE) and loading capacity (LC) of neo-antigens according to NP composition. Values are presented as mean ± SD of N=3, n=1. All NPs were produced with 10% (m/v) PVA, 2.5% (m/v) TPGS in internal and external phases, respectively. PVA and Pf-127 were used in the aqueous phase.

	MUT30[a]		**Mlmp3 D81N**[b]	
Nanoparticle matrix	EE[c] (%)	LC[d] (μg/mg)	EE[c] (%)	LC[d] (μg/mg)
PLA/PLGA	62.19 ± 8.01	31.10 ± 4.01	---	---
PLA/PLGA-Mannose	60.83 ± 6.54	30.42 ± 3.27	84.77 ± 9.09	42.38 ± 4.55
PLA/PLGA-PEG-Mannose	65.38 ± 9.22	32.69 ± 4.61	---	---

[a]MHCII MUT30 neo-antigen; [b]MHCI Mlmp3 D81N neo-antigen; [c]Entrapment efficiency; [d]Loading capacity

4.7 *In vivo* APCs internalization and maturation assay in C57BL/6J mice

Herein we show that NP composition affected DC internalization efficacy. The next crucial step was to assess the release profile of antigens from the NPs and the related activation of DCs, which will determine the therapeutic efficacy of the NPs. For that reason, Cy5-labelled NPs were injected subcutaneously to confirm their capacity to induce DC uptake (Figure 27 & 29) and maturation (Figure 28 & 30), prior to the evaluation of NP ability to induce a strong and specific immune response in the brain.

NPs tracking studies previously carried by our group revealed that the highest internalization of the DCs in the dLNs was obtained 17 h after immunization.

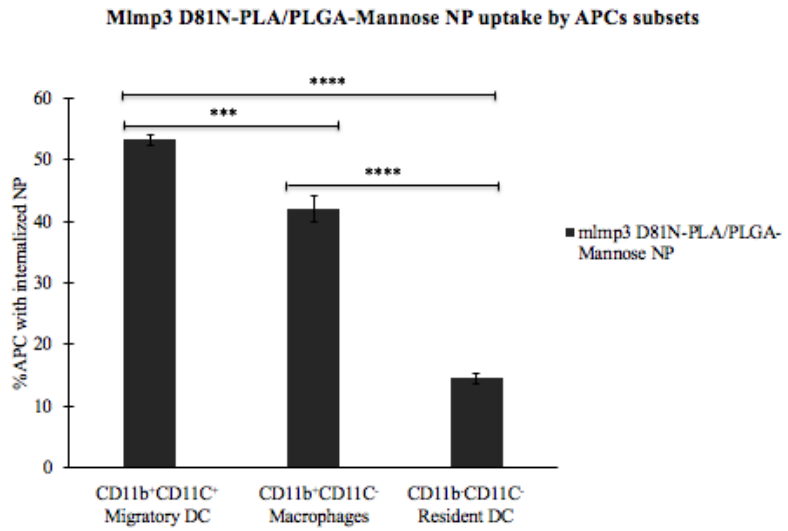

Figure 27 PLA/PLGA-Mannose NP containing glioblastoma neo-antigen was extensively internalized by migratory DC 17 h after inguinal LN immunization. Results were obtained by flow cytometer and the values are presented as mean ± SD, N=1, n=3. Ordinary one-way ANOVA followed by Tukey post-hoc test was used to compare PLA/PLGA-Mannose NP internalization by migratory DC, macrophages and resident DC. *** $p < 0.001$, **** $p < 0.0001$.

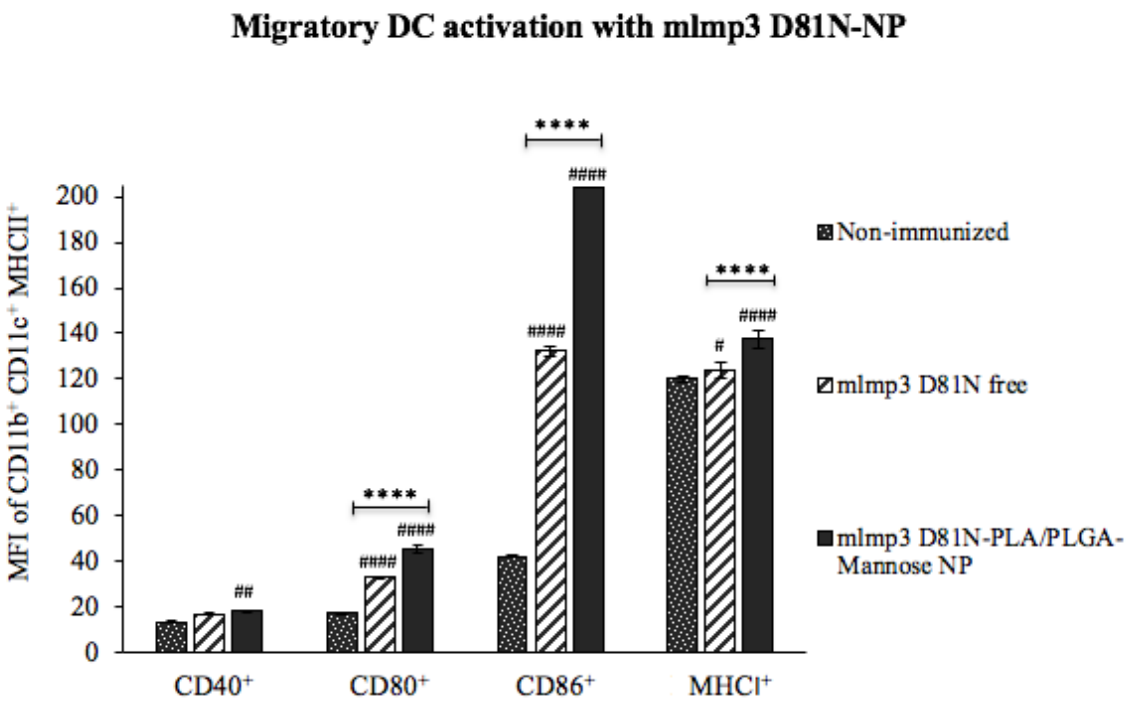

Figure 28 Activation of migratory DC 17 h upon immunization with PLA/PLGA-Mannose NP containing glioblastoma neo-antigen and adjuvants (Poly (I:C) and CpG). Results were obtained by flow cytometer and the values are presented as mean ± SD, N=1, n=3.Two-way ANOVA followed by Tukey post-hoc test were used to compare CD40, CD80, CD86 and MHC expression between free antigens and adjuvants and those entrapped in PLA/PLGA-Mannose NP. **** $p < 0.0001$ related to CD40, CD80, CD86 and MHC expression on cells collected from immunized animals. # $p < 0.05$, ## $p < 0.01$, ### $p < 0.0001$ related to the expression of CD40, CD80, CD86 and MHC of the controlled group collected from immunized animals.

Based on Figure 27 significant higher PLA/PLGA-Mannose NP internalization was observed in migratory DCs ($p \leq 0.0001$), followed by macrophages and resident DC.

Figure 28 shows a significantly higher expression of the activation markers on migratory DC surface with entrapped neo-antigen ($p < 0.0001$ for CD86, CD80, MHCI and $p = 0.0087$ in case of CD40), when compared to the neo-antigens and adjuvants in solution.

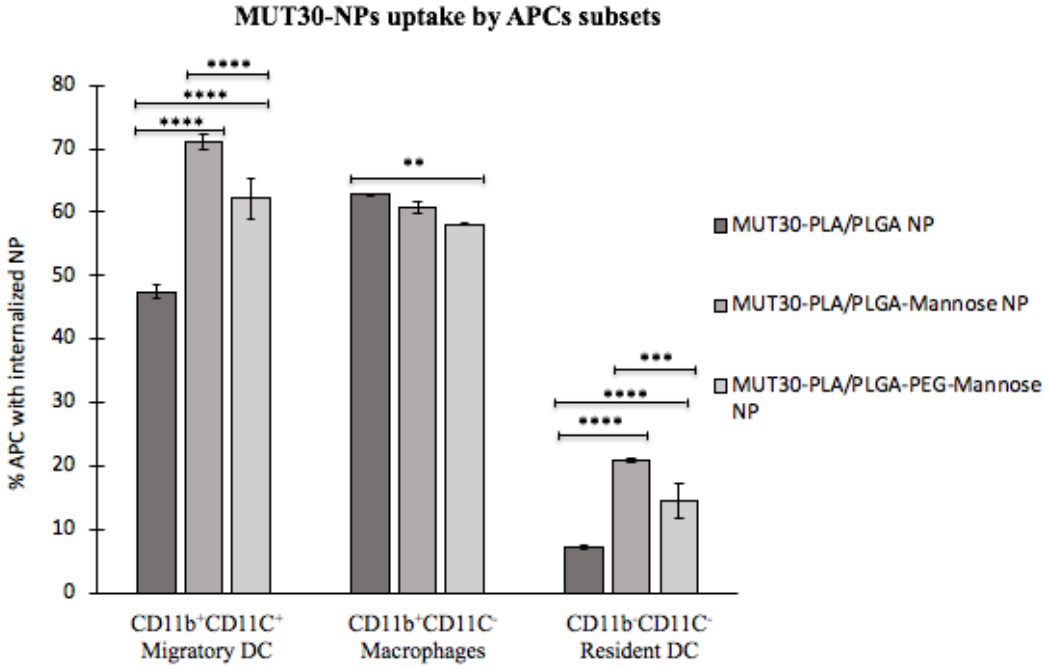

Figure 29 PLA/PLGA-Mannose NP containing melanoma neo-antigen and adjuvants (Poly (I:C) and CpG)) was extensively internalized by DCs 17 h after inguinal LN immunization. Results were obtained by flow cytometer and the values are presented as mean ± SD, N=1, n=3.Two-way ANOVA followed by Tukey post-hoc test were used to compare PLA/PLGA, PLA/PLGA-Mannose and PLA/PLGA-PEG-Mannose NPs internalization by migratory DC, macrophages and resident DC. ** $p < 0.01$, *** $p < 0.001$ **** $p < 0.0001$.

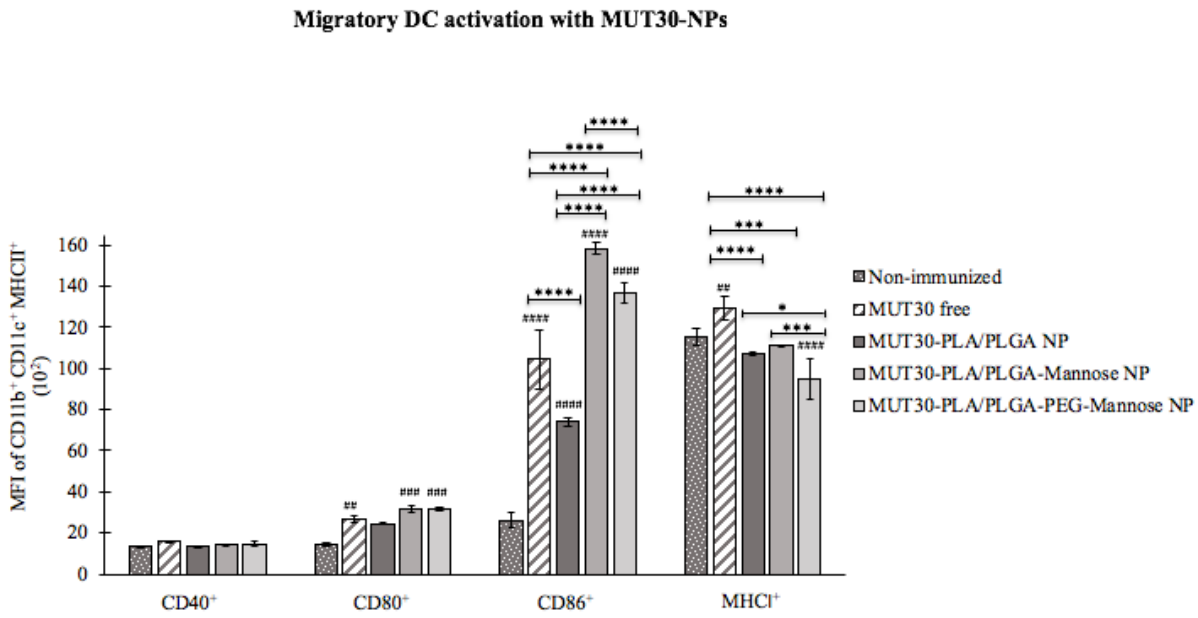

Figure 30 Activation of migratory DCs 17 h upon immunization with PLA/PLGA-Mannose NP containing melanoma neo-antigen and adjuvants (Poly (I:C) and CpG). Results were obtained by flow cytometer and the values are presented as mean ± SD, N=1, n=3.Two-way ANOVA followed by Tukey post-hoc test were used to compare CD40, CD80, CD86 and MHC expression between free antigens and adjuvants and those entrapped in particulate NPs, namely PLA/PLGA, PLA/PLGA-Mannose and PLA/PLGA-PEG-Mannose NPs ** p< 0.01, *** $p < 0.001$ **** $p < 0.0001$ related to CD80, CD86 and MHC expression on cells collected from immunized animals. ## p < 0.01, ### $p < 0.0001$ related to the expression of CD80, CD86 and MHC of the controlled group collected from immunized animals.

Based on Figure 30, significant higher PLA/PLGA-Mannose NP internalization was observed in both migratory and resident DC ($p \leq 0.0001$), when compared with PLA/PLGA-PEG-Mannose NP. No significant differences were observed between PLA/PLGA-Mannose and PLA/PLGA-PEG-Mannose NPs internalization by macrophages. PLA/PLGA NP was the least internalized by DC subpopulations ($p < 0.0001$).

According to Figure 30, there were no significant differences in the expression of CD80 and CD40 costimulatory markers for animals treated with the NPs and MUT30-ag and adjuvants administered in solution. The same figure shows a significantly higher expression of CD86 costimulatory signals on migratory DC surface by PLA/PLGA-Mannose NP when compared with other types of NPs and free group ($p < 0.0001$). Conversely MUT30-ag and adjuvants administered in solution promoted higher MHC expression when compared to the PLA/PLGA, PLA/PLGA-PEG-Mannose and PLA/PLGA-Mannose NPs ($p \leq 0.001$).

Chapter 5 - Discussion

Using NPs in immunotherapy is becoming worldwide recognized as one of the most promising techniques in cancer research. Understanding how NPs interact with the biological environment and how their physicochemical characteristics influence phagocytic recognition, uptake and toxicological effects allows researchers to design more effective nanoparticulate delivery systems.

The aim of this study was to develop a nanodelivery system capable of targeting DCs cells and promoting DCs activation and maturation to further potentiate the immune cell effector function towards malignant cells in the brain. We also intended to understand how differences in the NP composition could affect NP-DC interaction.

We developed different biodegradable and biocompatible NPs with i) PEG to reduce NPs immunogenicity, such as PLGA-PEG and PLA/PLGA-PEG NPs, ii) mannose to target the MR/CD206 on APCs, such as PLA/PLGA-PEG-Mannose and PLA/PLGA-Mannose NPs and iii) PLA/PLGA NP to study the non-specific DCs internalization. The aim was to study how differences in NPs surface functionalization could impact DCs internalization.

In the first part of this project, three biodegradable and biocompatible nanoparticulate systems were developed, based on PLGA-PEG, PLA/PLGA-PEG and PLA/PLGA-PEG-Mannose polymer blend. These nanovaccines candidates presented physicochemical properties adequate for DC targeting, with an average size below 200 nm, narrow particle size distribution and spherical-shaped particles.

All NP systems presented negatively charged surfaces, which might indicate that PEG chains were not sufficient to shield the negative surface charge of PLGA NPs[83]. Indeed the amount of PLGA in PLGA-PEG NP is higher than the one used for the development of the other NP formulations, which leads to higher amounts of carboxyl end groups on NP surface and therefore, in a more negatively charged surface. The size of the PLA/PLGA-PEG NP was smaller than those obtained for PLGA-PEG and PLA/PLGA-PEG-Mannose NPs. According to Conniot *et al.* (2019), adding mannose onto NP surface (PLA/PLGA and PLA/PLGA-Mannose) does not influence NP size. Therefore, it was not expected to obtain differences in the mean size of PLA/PLGA-PEG and PLA/PLGA-PEG-Mannose NPs.

Regarding the size and morphology analyzed by AFM, all NPs presented spherical and slightly rough surface. Both PLGA-PEG and PLA/PLGA-PEG NPs presented an average NP diameter smaller than the hydrodynamic diameter obtained by DLS, which was expected and it can be explained by the absence of NP hydration. However, AFM images of PLA/PLGA-

PEG-Mannose showed an average diameter higher than the one obtained by DLS, as well as a wider particle size distribution. Thus, AFM results did not coincide with published results, where it is described a smaller hydrodynamic diameter than the one obtained in DLS.

Another conclusion that we can take from the AFM images is a clear distinction in NPs boundaries. NPs containing less amount of PEG showed a sharp imaging of particle limits, while this was very hard to see in PLGA-PEG NPs. These results suggest that the amount of water bound to PEG chains was not efficiently dried.

Before administering NPs to effectively target APCs and subsequently disrupt the endosome to release the loaded peptides into APCs cytosol, NPs stability was evaluated. NPs size and surface charge were followed for seven weeks in PBS pH 7.4 at 37°C, due to its similarity to physiological conditions. The effect of different temperatures on the properties of NP was also studied.

After three weeks, a drastic increase in PLGA-PEG NP size and PdI was detected, suggesting a faster polymer degradation[107]. Comparing PLA/PLGA-PEG with PLA/PLGA-PEG-Mannose NPs, no significant changes in size or PdI were shown for seven weeks. This stability could be explained by steric hindrance and repulsion of hydrophilic PEG chains[129]. Comparing the surface charge along time, all NPs became less negative at higher temperatures, with changes being more evident in PLGA-PEG NP, which showed a reverse on NP surface charge from negative values to almost neutral ones. Both PLA/PLGA-PEG and PLA/PLGA-PEG-Mannose NPs exhibited a decrease on their surface charge but continued to be more negative than PLGA-PEG NP.

At 4 °C, the surface charge and size of all NPs were not changed over time. NPs stored at 4 °C presented smaller mean diameters than those obtained upon NP incubation at 37°C. In this sense, storage temperature is important to maintain the integrity of these delivery systems[130].

In an attempt to mimic the endosome compartment conditions (pH ~4.5 – 6.5)[85] and thus NP degradation following their internalization, NPs were suspended in PBS pH 5.7 at 37°C. Since the acidic pH triggers protonation of the carboxyl groups, and thereby the switch of PLGA negative surface charge to neutral or even positive values, and hence promote antigen release into the cytosol, we were expecting differences in NP degradation according to matrix composition (PLGA and PLA NPs)[19].

Similarly to the stability assay for PLGA-PEG NP in pH 7.4, we also observed a drastic increase in PLGA-PEG NP size and a decrease on surface charge over time, which is consistent

with the degradation of the aliphatic polyesters and exposure of an increasing number of carboxylic groups. Since at both pH conditions, the size and PdI of PLGA-PEG NP increased and the surface charge decreased, our results showed that the PLGA-PEG NP degradation was not strongly affected by pH. Yet, PLGA degradation is known to be effect by acidic conditions[131].

On the other hand, the acidic pH triggered a more significant change in PLA/PLGA-PEG and PLA/PLGA-PEG-Mannose NPs surface charges. Regarding the last two weeks of the stability study, PLA/PLGA-PEG NP size increased, which might indicate their degradation. According to the literature, pH, temperature and autocatalysis determines PLA degradation rate. It is reported a faster PLA degradation process in highly basic and highly acidic mediums, when compared to neutral pH[87]. Still, PLA NPs reveled to be more stable than PLGA-PEG NP due to the higher hydrophobicity of the lactic acid and thus lower hydrolysis rate[60].

To confirm NP degradation process, molecular weight and loss of mechanical strength of the polymer matrix could have been monitored. Polymers can be degraded by random chain scission to lower the Mw of small chains. It has also been noted that the crystallinity of PLA tends to increase as it degrades. Thus, determining the crystallinity of NPs in the early stages and by the end of the seven weeks could also be used as a supplementary tool to assess the progress of degradation. As the accumulation of PLGA monomers along polymer degradation leads to lower pH values, pH medium could also have been monitored[87,89].

The cell viability was performed *in vitro* with murine immature DC cell line (JAWSII) through MTT assay and flow cytometry. The cells were incubated for 96 h with increasing NPs concentrations (0.25 – 1 mg/ml). This quantitative colorimetric test showed that the cell viability was not affected by NP composition (cell viability > 80%) up to 1 mg/mL. All cells exhibited a normal metabolic activity and could metabolize the water-soluble dye (MTT) into a colored insoluble formazan salt[132]. To confirm that the NPs did not compromise cell viability, the integrity of DNA was also evaluated by staining immature DC with PI, an apoptosis marker. It is based on the principle that apoptotic cells have their DNA fragmentated and, consequently, lose nuclear DNA content. DNA content is measured by flow cytometry, after DNA being stained with PI[133]. Again, this essay showed that the cell viability was not affected by the composition of NPs at 0.5 mg/mL (cell viability > 90%), highlighting the safety of these NPs.

To assess if the produced NPs were internalized by APCs, JAWSII cells were incubated with Cy5-labelled NPs. The results showed that DCs internalized both PLA/PLGA-PEG and PLA/PLGA-PEG-Mannose NPs at a higher extent than the PLGA-PEG NP. Looking into the cellular uptake kinetics and comparing those with the literature, higher DCs uptake values were

expected for NP functionalized with mannose due to the interaction of this targeting moiety with the MR/CD206 receptor at the DCs surface. However, based on the results obtained, PLA/PLGA-PEG NP presented higher MFI values, which correspond to higher internalization into the murine immature DCs than the PLA/PLGA-PEG-Mannose NP.

On the other hand, PLGA-PEG NP showed a delay in their internalization by DCs, which may be explained by both surface hydration (i.e. formation of a hydration layer on NPs surface) and PEO chains flexibility (i.e. steric repulsion) that protects NP surface and further particle–cell interactions[134].

Prior to entrapping the selected neo-antigens in NPs for *in vivo* studies, ovalbumin (OVA) was loaded as a model antigen in PLA/PLGA-PEG-Mannose NP. PLA/PLGA-PEG-Mannose NP was selected among others once it has mannose on its surface to target the CD206 APCs surface receptors. PLA/PLGA-PEG-Mannose NP was able to entrap OVA protein with high EE. Since OVA protein has higher MW than the glioblastoma and melanoma neo-antigens that we will use in APC activation study, it is expected that the developed NP could entrap those neo-antigens.

Since the PLA-based NPs (PLA/PLGA-PEG and PLA/PLGA-PEG-Mannose) have shown more promising results regarding DC uptake, we decided to study the PLA-based NPs (PLA/PLGA, PLA/PLGA-Mannose and PLA/PLGA-PEG-Mannose) ability to induce *in vivo* DCs activation and maturation.

In a study conducted by Conniot and colleagues (2019), PLA/PLGA and PLA/PLGA-Mannose NPs were produced with 0.25% (m/v) PVA in the final phase. Those NPs were deeply characterized in terms of size, PdI, zeta-potential and morphology and had shown to be non cytotoxic[127]. Plus, in the same study, the produced NPs showed to be capable of entrapping both MHCI and MHCII antigens with high EE (97.5 ± 0.2% and 74.6 ± 3.5%, respectively) as well as LC (48.8 ± 0.1 μg/mg and 75.6 ± 3.5 μg/mg, respectively)[127]. Based on those results, it was not necessary to physiochemically characterize PLA/PLGA and PLA/PLGA-Mannose NPs once again as well as NPs capacity to encapsulate OVA model antigen, as the capacity of NPs encapsulation was previously described. Together these results suggest that PLA/PLGA and PLA/PLGA-Mannose NPs have adequate NP characteristics for targeting DCs and can be used in *in vivo* assays.

Concerning PLA/PLGA-PEG-Mannose NP, as it was already characterized and proved to be capable of being internalized without compromising cell viability and could entrap OVA antigen, this NP was also used in *in vivo* studies.

Based on the effect that PF-127 has on NPs stability and its capacity to generate small NPs, PF-127 was tested in the final phase of PLA/PLGA and PLA/PLGA-Mannose NPs. Since change in the aqueous phase may change the characteristics of the NPs[135], NPs physicochemical properties were characterized prior to the *in vivo* studies.

Comparing the physicochemical properties of PLA/PLGA NP prepared in Conniot *et al.* (2019) study with the data obtained prepared with PF-127, the latter showed higher mean size (214 ± 2.9 and 168 ± 10 nm, respectively). Because changes in zeta-potential of PLA/PLGA NP prepared with PF-127 were not significant, using PF-127 instead of PVA did not influence NP surface charge. MUT30-PLA/PLGA NP presented similar hydrodynamic diameter and zeta-potential values as plain PLA/PLGA NP (i.e. NP deprived of any payload). In this scenario, MUT30 neo-antigen entrapment did not influence hydrodynamic diameter and surface charge of PLA/PLGA NP.

Looking into plain PLA/PLGA-Mannose NPs prepared with PVA and PF-127 in the aqueous phase, the size of PLA/PLGA-Mannose NP prepared with PF-127 was not affected whereas surface charge increased when compared with the one prepared with PVA (-14.5 ± 0.53 mV from -3.29 ± 0.34 mV, respectively) (Table 5). No alterations were expected on NP surface charge using PF-127 since it is a non-ionic polymer and therefore do not have any charge at physiological pH. MUT30-PLA/PLGA-Mannose NP presented slightly higher hydrodynamic diameter and PdI than plain PLA/PLG-Mannose NP while surface charge was not affected. Differences in mlmp3 D81N-PLA/PLGA-Mannose and plain PLA/PLGA-Mannose NPs mean size, PdI and zeta-potential were not shown. Nevertheless, both PLA/PLGA and PLA/PLGA-Mannose NPs efficiently entrap the neo-antigen.

Looking into the plain PLA/PLGA-Mannose and plain PLA/PLGA-PEG-Mannose, both formulated with PVA in the aqueous phase, presented similar hydrodynamic diameter. Since PEG provides steric repulsion, it would be expected that the NPs prepared with this polymer exhibited smaller mean size. Nevertheless, it was not verified. Comparing the surface charge of PLA/PLGA-PEG-Mannose and PLA/PLGA-Mannose, no significant changes were observed. Again, it would be expected to see an effect of PEG in PLA/PLGA-PEG-Mannose NP surface charge, once PEG can shield the negative surface charge of PLGA polymer.

Together, all the PLA-based NPs with PF-127 and PVA in the final phase presented physicochemical properties adequate for DC targeting, with an average size close to 200 nm, narrow particle size distribution and neutral negative charge.

All the designed NPs used for APCs maturation study (PLA/PLGA, PLA/PLGA-Mannose and PLA/PLGA-PEG-Mannose) were internalized by migratory DC at higher extent than by macrophages and resident DC. Comparing PLA/PLGA-Mannose and PLA/PLGA-PEG-Mannose NPs, PLA/PLGA-Mannose NP was significantly more internalized both in migratory and resident DCs, whereas in macrophages significant changes in the internalization were not observed between the two formulations.

To access the effect of different NPs formulations containing tumor neo-antigens and TLR ligands Poly(I:C) and CpG on the induction of migratory DCs maturation, the analysis of CD40, CD80, CD86 and MHC expression was conducted after animals' immunization.

When comparing PLA/PLGA-Mannose NP entrapping mlmp3 D81N and adjuvants and the same peptides in solution, migratory DC expressed significantly higher expression of costimulatory molecules and MHCI levels after vaccination with PLA/PLGA-Mannose NP, which demonstrates the importance of using NPs as vaccine delivery systems. The entrapment of antigens and adjuvants into NPs aims to enhance immunogenicity by preventing peptide degradation and enhancing their uptake by APCs and further activation. Peptides in NPs are more immunogenic than in their free form[136].

Concerning DC internalization, PLA/PLGA-Mannose NP was higher internalized in both migratory and resident DC than PLA/PLGA-PEG-Mannose NP. No significant changes in macrophages internalization were seen between them.

In DC activation study with MUT30-NPs, migratory DC treated with PLA/PLGA-Mannose NP showed a marked increase in CD86 and MHCI expression comparing with PLA/PLGA-PEG-Mannose NP. Since after immunization with PLA/PLGA-Mannose and PLA/PLGA-PEG-Mannose NPs, migratory DCs showed similar expression of CD40 and CD80 maturation markers and taking into consideration the previous CD86 and MHCI expression results, functionalizing NP surface with PEG showed to be non-advantageous for this study at this time point. With this, we hypothesize that the ratio of PEG and Mannose used for this study may not be optimize. Maybe, functionalizing NP with di-mannose may enhance the expression of key surface markers that are associated with DC maturation and antigen presentation[137].

Comparing PLA/PLGA and PLA/PLGA-Mannose NPs, PLA/PLGA NP exhibited lower costimulatory molecules expression, which might indicate the added value of the mannose ligand on DCs maturation[137].

After animals's immunization with MUT30 and adjuvants in free form, migratory DC expressed significantly higher levels of MHCI over all particulate systems. This outcome may

be explained by the fact that free antigens do not depend on polymer degradation and further release, to be presented to MHC complex. According to the literature, entrapping tumor neo-antigens into PLGA NPs are advantageous because they may provide controlled and sustained release. So we hypothesized that a longer time of incubation would be necessary to see a higher effect of these NPs on MHCI expression.

In both maturation studies differences in the CD80 and CD86 expression might be explained by the fact that the induction of the CD86 expression molecules happens in different moments of the DC maturation process. CD80 is slowly induced but remains stable for a longer period of time, while CD86 is induced at an early stage upon stimulation, but its expression starts to decrease 48 h after the stimulus[138,139].

Chapter 6 – Conclusion & future perspectives

This work describes the development and characterization of non-toxic biodegradable (poly(lactic-co-glycolic acid) (PLGA) NPs to study the impact that these NP composition will have in DCs internalization and further activation. Several NPs were developed with different polymer composition: non-targeted poly(lactic acid)/poly(lactic-co-glycolic acid)-pol(ethylene glycol) (PLA/PLGA-PEG) NP, PLGA-PEG and PLA/PLGA NPs, or targeted PLA/PLGA-PEG-mannose and PLA/PLGA-Mannose NPs to increase recognition and further internalization mediated by the mannose receptor at DC surface.

Overall, the data present herein highlights the importance of the composition and the physicochemical properties of nanoparticulate vaccines in DC cellular uptake and maturation, with more focus on PLA-based NPs. It was possible to observe that functionalizing NP with mannose enhanced the expression of CD80 and CD86 surface markers and MHC molecule that are associated with DC maturation and antigen presentation. These results suggest that mannose functionalization can significantly increase the induction of the maturation process of DCs, which may happen due to an increase of the uptake of the mannose-functionalized NPs, but also to its intrinsic immunoadjuvant effect, translating the great potential of the developed NPs to be used as a cancer vaccine. Also, comparing the results between PLA/PLGA-Mannose and PLA/PLGA-PEG-Mannose NPs in DCs internalization, we can conclude that NP functionalized with PEG did not conferred any advantage and so, we hypothesized increasing the ratio of PEG and Mannose (di-mannose) to see higher DCs internalization or even changing PEG for other hydrophilic coating polymer like poly(oxazoline) (Pox).

Considering the results obtained during the project, it should be evaluate the ability of NPs to induce T cell activation and proliferation. Having into consideration that we plan to characterize the anti-tumor immune-mediated effect induced by our nanovaccines, mice would be euthanized, and CTL responses would be quantified. This would involve the quantification of molecules involved in tumor apoptosis, such as granzymes and membrane-disrupting protein perforin, Fas and FasL and IFN expression. $CD4^+$ T cells activity could also be studied since it recruits cells from the innate immune system such as NK cells, granulocytes or macrophages that also contribute to tumor cell lysis.

In addition, as MDSCs subsets in TME have been described to participate in immunosuppression, we would assess the presence of MDSCs within the TME before and after

NP treatment to evaluate the possible infiltration of immunosuppressive cells that NP might have induced.

Chapter 7 - References

1. Dinarvand, R., Sepehri, N., Manouchehri, Rouhani & Atyabi, F. Polylactide-co-glycolide nanoparticles for controlled delivery of anticancer agents. *Int. J. Nanomedicine* **6**, 877 (2011).
2. Conniot, J. *et al.* Cancer immunotherapy: nanodelivery approaches for immune cell targeting and tracking. *Front. Chem.* **2**, 1–27 (2014).
3. Vienne-Jumeau, A., Tafani, C. & Ricard, D. Environmental risk factors of primary brain tumors: A review. *Rev. Neurol. (Paris).* (2019). doi:10.1016/j.neurol.2019.08.004
4. Tandel, G. S. *et al.* A Review on a Deep Learning Perspective in Brain Cancer Classification. *Cancers (Basel).* **11**, 111 (2019).
5. Maher, E. A. & Bachoo, R. M. Glioblastoma. in *Rosenberg's Molecular and Genetic Basis of Neurological and Psychiatric Disease* 909–917 (Elsevier, 2015). doi:10.1016/B978-0-12-410529-4.00078-4
6. Vosoughi, E. *et al.* Survival and clinical outcomes of patients with melanoma brain metastasis in the era of checkpoint inhibitors and targeted therapies. *BMC Cancer* **18**, 490 (2018).
7. Ali, Z., Yousaf, N. & Larkin, J. Melanoma epidemiology, biology and prognosis. *Eur. J. Cancer Suppl.* **11**, 81–91 (2013).
8. Pitcovski, J., Shahar, E., Aizenshtein, E. & Gorodetsky, R. Melanoma antigens and related immunological markers. *Crit. Rev. Oncol. Hematol.* **115**, 36–49 (2017).
9. Abate-Daga, D., Ramello, M. C., Smalley, I., Forsyth, P. A. & Smalley, K. S. M. The biology and therapeutic management of melanoma brain metastases. *Biochem. Pharmacol.* **153**, 35–45 (2018).
10. Uong, A. & Zon, L. I. Melanocytes in development and cancer. *J. Cell. Physiol.* **222**, 38–41 (2010).
11. Shanmuganathan, R. *et al.* Chitosan nanopolymers: An overview of drug delivery against cancer. *Int. J. Biol. Macromol.* **130**, 727–736 (2019).
12. Chu, L. *et al.* Nose-to-brain delivery of temozolomide-loaded PLGA nanoparticles functionalized with anti-EPHA3 for glioblastoma targeting. *Drug Deliv.* **25**, 1634–1641 (2018).
13. Chaudhuri, T. R. & Straubinger, R. M. Nanoparticles for Brain Tumor Delivery. in *Nervous System Drug Delivery* 229–250 (Elsevier, 2019). doi:10.1016/B978-0-12-813997-4.00012-8
14. Li, Y. D. *et al.* Tumor-induced peripheral immunosuppression promotes brain metastasis in patients with non-small cell lung cancer. *Cancer Immunol. Immunother.* **68**, 1501–1513 (2019).
15. Ward, J. P., Gubin, M. M. & Schreiber, R. D. The Role of Neoantigens in Naturally Occurring and Therapeutically Induced Immune Responses to Cancer. in *Advances in Immunology* **130**, 25–74 (Elsevier Inc., 2016).
16. Escribese, M. M. & Barber, D. New insight into cancer immunotherapy. *Allergol. Immunopathol. (Madr).* **45**, 50–55 (2017).
17. Dudek, A. M., Martin, S., Garg, A. D. & Agostinis, P. Immature, Semi-Mature, and Fully Mature Dendritic Cells: Toward a DC-Cancer Cells Interface That Augments Anticancer Immunity. *Front. Immunol.* **4**, (2013).
18. Antonios, J. P., Everson, R. G. & Liau, L. M. Dendritic cell immunotherapy for brain tumors. *J. Neurooncol.* **123**, 425–432 (2015).
19. Silva, J. M., Videira, M., Gaspar, R., Préat, V. & Florindo, H. F. Immune system targeting by biodegradable nanoparticles for cancer vaccines. *J. Control. Release* **168**,

179–199 (2013).
20. Song, C. *et al.* Recent Advances in Particulate Adjuvants for Cancer Vaccination. *Adv. Ther.* **3**, 18 (2019).
21. McCarthy, D. P., Hunter, Z. N., Chackerian, B., Shea, L. D. & Miller, S. D. Targeted immunomodulation using antigen-conjugated nanoparticles. *Wiley Interdiscip. Rev. Nanomedicine Nanobiotechnology* **6**, 298–315 (2014).
22. Silva, A. L. *et al.* Nanoparticle impact on innate immune cell pattern-recognition receptors and inflammasomes activation. *Semin. Immunol.* **34**, 3–24 (2017).
23. Magee, C. N., Boenisch, O. & Najafian, N. The Role of Costimulatory Molecules in Directing the Functional Differentiation of Alloreactive T Helper Cells. *Am. J. Transplant.* **12**, 2588–2600 (2012).
24. Aqbi, H. F., Wallace, M., Sappal, S., Payne, K. K. & Manjili, M. H. IFN-γ orchestrates tumor elimination, tumor dormancy, tumor escape, and progression. *J. Leukoc. Biol.* **103**, 1219–1223 (2018).
25. Wong, R. S. Y. Apoptosis in cancer: from pathogenesis to treatment. *J. Exp. Clin. Cancer Res.* **30**, 87 (2011).
26. Ratajczak, W., Niedźwiedzka-Rystwej, P., Tokarz-Deptuła, B. & Deptuła, W. Immunological memory cells. *Cent. Eur. J. Immunol.* **43**, 194–203 (2018).
27. Garbi, N. & Kreutzberg, T. Dendritic cells enhance the antigen sensitivity of T cells. *Front. Immunol.* **3**, 1–10 (2012).
28. Irvine, D. J., Swartz, M. A. & Szeto, G. L. Engineering synthetic vaccines using cues from natural immunity. *Nat. Mater.* **12**, 978–990 (2013).
29. Torgovnick, A. & Schumacher, B. DNA repair mechanisms in cancer development and therapy. *Front. Genet.* **6**, 1–15 (2015).
30. TYSNES, B. & BJERKVIG, R. Cancer initiation and progression: Involvement of stem cells and the microenvironment. *Biochim. Biophys. Acta - Rev. Cancer* **1775**, 283–297 (2007).
31. Gacche, R. N. & Assaraf, Y. G. Redundant angiogenic signaling and tumor drug resistance. *Drug Resist. Updat.* **36**, 47–76 (2018).
32. De Sanctis, F., Ugel, S., Facciponte, J. & Facciabene, A. The dark side of tumor-associated endothelial cells. *Semin. Immunol.* **35**, 35–47 (2018).
33. Schaaf, M. B., Garg, A. D. & Agostinis, P. Defining the role of the tumor vasculature in antitumor immunity and immunotherapy. *Cell Death Dis.* **9**, 115 (2018).
34. Belli, C. *et al.* Targeting the microenvironment in solid tumors. *Cancer Treat. Rev.* **65**, 22–32 (2018).
35. Nabil, G. *et al.* Nanoengineered delivery systems for cancer imaging and therapy: recent advances, future directions and patent evaluation. *Drug Discov. Today* **6446**, (2018).
36. Roskoski, R. Vascular endothelial growth factor (VEGF) signaling in tumor progression. *Crit. Rev. Oncol. Hematol.* **62**, 179–213 (2007).
37. Ma, Q., Dieterich, L. C. & Detmar, M. Multiple roles of lymphatic vessels in tumor progression. *Curr. Opin. Immunol.* **53**, 7–12 (2018).
38. Shrimali, R. K. *et al.* Antiangiogenic agents can increase lymphocyte infiltration into tumor and enhance the effectiveness of adoptive immunotherapy of cancer. *Cancer Res.* **70**, 6171–6180 (2010).
39. Darvin, P., Toor, S. M., Sasidharan Nair, V. & Elkord, E. Immune checkpoint inhibitors: recent progress and potential biomarkers. *Exp. Mol. Med.* **50**, 165 (2018).
40. Greten, T. F. & Sangro, B. Targets for immunotherapy of liver cancer. *J. Hepatol.* **68**, 157–166 (2018).
41. Saeidi, A. *et al.* T-Cell Exhaustion in Chronic Infections: Reversing the State of

Exhaustion and Reinvigorating Optimal Protective Immune Responses. *Front. Immunol.* **9**, 1–12 (2018).
42. Kircher, D., Silvis, M., Cho, J. & Holmen, S. Melanoma Brain Metastasis: Mechanisms, Models, and Medicine. *Int. J. Mol. Sci.* **17**, 1468 (2016).
43. Lyon, J. G., Mokarram, N., Saxena, T., Carroll, S. L. & Bellamkonda, R. V. Engineering challenges for brain tumor immunotherapy. *Adv. Drug Deliv. Rev.* **114**, 19–32 (2017).
44. Sonvico, F. *et al.* Surface-Modified Nanocarriers for Nose-to-Brain Delivery: From Bioadhesion to Targeting. *Pharmaceutics* **10**, 34 (2018).
45. Kimiz-Gebologlu, I., Gulce-Iz, S. & Biray-Avci, C. Monoclonal antibodies in cancer immunotherapy. *Mol. Biol. Rep.* **45**, 2935–2940 (2018).
46. Liddell, E. Antibodies. in *The Immunoassay Handbook* **1**, 245–265 (Elsevier, 2013).
47. Pardoll, D. M. The blockade of immune checkpoints in cancer immunotherapy. *Nat. Rev. Cancer* **12**, 252–264 (2012).
48. Naing, A. *et al.* Anti-PD-1 monoclonal antibody MEDI0680 in a phase I study of patients with advanced solid malignancies. *J. Immunother. Cancer* **7**, 225 (2019).
49. Dunn, G. P., Fecci, P. E. & Curry, W. T. Cancer Immunoediting in Malignant Glioma. *Neurosurgery* **71**, 201–223 (2012).
50. Vacchelli, E. *et al.* Trial watch: Peptide vaccines in cancer therapy. *Oncoimmunology* **1**, 1557–1576 (2012).
51. Lee, C., Yelensky, R., Jooss, K. & Chan, T. A. Update on Tumor Neoantigens and Their Utility: Why It Is Good to Be Different. *Trends Immunol.* **xx**, 1–13 (2018).
52. Grenier, J. M., Yeung, S. T. & Khanna, K. M. Combination Immunotherapy: Taking Cancer Vaccines to the Next Level. *Front. Immunol.* **9**, 1–9 (2018).
53. Peng, M. *et al.* Neoantigen vaccine: an emerging tumor immunotherapy. *Mol. Cancer* **18**, 128 (2019).
54. Li, L., Goedegebuure, S. P. & Gillanders, W. E. Preclinical and clinical development of neoantigen vaccines. *Ann. Oncol.* **28**, xii11–xii17 (2017).
55. Guo, Y., Lei, K. & Tang, L. Neoantigen Vaccine Delivery for Personalized Anticancer Immunotherapy. *Front. Immunol.* **9**, 1–8 (2018).
56. Blanchet, J.-S. *et al.* A New Generation of Melan-A/MART-1 Peptides That Fulfill Both Increased Immunogenicity and High Resistance to Biodegradation: Implication for Molecular Anti-Melanoma Immunotherapy. *J. Immunol.* **167**, 5852–5861 (2001).
57. Ma, W. *et al.* PLGA nanoparticle-mediated delivery of tumor antigenic peptides elicits effective immune responses. *Int. J. Nanomedicine* **7**, 1475 (2012).
58. Warrier, V. U. *et al.* Engineering anti-cancer nanovaccine based on antigen cross-presentation. *Biosci. Rep.* **39**, 1–19 (2019).
59. Comberlato, A., Paloja, K. & Bastings, M. M. C. Nucleic acids presenting polymer nanomaterials as vaccine adjuvants. *J. Mater. Chem. B* **7**, 6321–6346 (2019).
60. Allahyari, M. & Mohit, E. Peptide/protein vaccine delivery system based on PLGA particles. *Hum. Vaccin. Immunother.* **12**, 806–828 (2016).
61. Ammi, R. *et al.* Poly(I:C) as cancer vaccine adjuvant: Knocking on the door of medical breakthroughs. *Pharmacol. Ther.* **146**, 120–131 (2015).
62. Zhao, X. *et al.* Poly I:C-Induced Tumor Cell Apoptosis Mediated by Pattern-Recognition Receptors. *Cancer Biother. Radiopharm.* **27**, 530–534 (2012).
63. Oliveira, M. F., Guimarães, P. P. G., Gomes, A. D. M., Suárez, D. & Sinisterra, R. D. Strategies to target tumors using nanodelivery systems based on biodegradable polymers, aspects of intellectual property, and market. *J. Chem. Biol.* **6**, 7–23 (2013).
64. Peres, C. *et al.* Poly(lactic acid)-based particulate systems are promising tools for immune modulation. *Acta Biomater.* **48**, 41–57 (2017).

65. Giuliano, E., Paolino, D., Fresta, M. & Cosco, D. Drug-Loaded Biocompatible Nanocarriers Embedded in Poloxamer 407 Hydrogels as Therapeutic Formulations. *Medicines* **6**, 7 (2018).
66. Yildirimer, L., Thanh, N. T. K., Loizidou, M. & Seifalian, A. M. Toxicology and clinical potential of nanoparticles. *Nano Today* **6**, 585–607 (2011).
67. Baetke, S. C., Lammers, T. & Kiessling, F. Applications of nanoparticles for diagnosis and therapy of cancer. *Br. J. Radiol.* **88**, 20150207 (2015).
68. Cho, K., Wang, X., Nie, S., Chen, Z. & Shin, D. M. Therapeutic Nanoparticles for Drug Delivery in Cancer. *Clin. Cancer Res.* **14**, 1310–1316 (2008).
69. Li, Z., Tan, S., Li, S., Shen, Q. & Wang, K. Cancer drug delivery in the nano era: An overview and perspectives. *Oncol. Rep.* **38**, 611–624 (2017).
70. Huang, Y.-Z., Gao, J.-Q., Liang, W.-Q. & Nakagawa, S. Preparation and Characterization of Liposomes Encapsulating Chitosan Nanoparticles. *Biol. Pharm. Bull.* **28**, 387–390 (2005).
71. Torchilin, V. P. Micellar Nanocarriers: Pharmaceutical Perspectives. *Pharm. Res.* **24**, 1–16 (2006).
72. Mansour, H. M., Sohn, M., Al-Ghananeem, A. & DeLuca, P. P. Materials for Pharmaceutical Dosage Forms: Molecular Pharmaceutics and Controlled Release Drug Delivery Aspects. *Int. J. Mol. Sci.* **11**, 3298–3322 (2010).
73. Xiong, X.-B., Falamarzian, A., Garg, S. M. & Lavasanifar, A. Engineering of amphiphilic block copolymers for polymeric micellar drug and gene delivery. *J. Control. Release* **155**, 248–261 (2011).
74. Lu, Y. & Park, K. Polymeric micelles and alternative nanonized delivery vehicles for poorly soluble drugs. *Int. J. Pharm.* **453**, 198–214 (2013).
75. Rohovie, M. J., Nagasawa, M. & Swartz, J. R. Virus-like particles: Next-generation nanoparticles for targeted therapeutic delivery. *Bioeng. Transl. Med.* **2**, 43–57 (2017).
76. Ong, H. K., Tan, W. S. & Ho, K. L. Virus like particles as a platform for cancer vaccine development. *PeerJ* **5**, e4053 (2017).
77. Hossen, S. *et al.* Smart nanocarrier-based drug delivery systems for cancer therapy and toxicity studies: A review. *J. Adv. Res.* **15**, 1–18 (2019).
78. Cheng, Y., Zhao, L., Li, Y. & Xu, T. Design of biocompatible dendrimers for cancer diagnosis and therapy: current status and future perspectives. *Chem. Soc. Rev.* **40**, 2673 (2011).
79. Yang, H. Targeted nanosystems: Advances in targeted dendrimers for cancer therapy. *Nanomedicine Nanotechnology, Biol. Med.* **12**, 309–316 (2016).
80. Khandare, J., Calderón, M., Dagia, N. M. & Haag, R. Multifunctional dendritic polymers in nanomedicine: opportunities and challenges. *Chem. Soc. Rev.* **41**, 2824–2848 (2012).
81. Artiga, Á., Serrano-Sevilla, I., De Matteis, L., Mitchell, S. G. & de la Fuente, J. M. Current status and future perspectives of gold nanoparticle vectors for siRNA delivery. *J. Mater. Chem. B* **7**, 876–896 (2019).
82. Evans, E. R., Bugga, P., Asthana, V. & Drezek, R. Metallic nanoparticles for cancer immunotherapy. *Mater. Today* **21**, 673–685 (2018).
83. Silva, J. M. *et al.* In vivo delivery of peptides and Toll-like receptor ligands by mannose-functionalized polymeric nanoparticles induces prophylactic and therapeutic anti-tumor immune responses in a melanoma model. *J. Control. Release* **198**, 91–103 (2015).
84. Moon, J. J., Huang, B. & Irvine, D. J. Engineering Nano- and Microparticles to Tune Immunity. *Adv. Mater.* **24**, 3724–3746 (2012).
85. Silva, A. L., Soema, P. C., Slütter, B., Ossendorp, F. & Jiskoot, W. PLGA particulate

delivery systems for subunit vaccines: Linking particle properties to immunogenicity. *Hum. Vaccin. Immunother.* **12**, 1056–1069 (2016).
86. Yan, F. *et al.* The effect of poloxamer 188 on nanoparticle morphology, size, cancer cell uptake, and cytotoxicity. *Nanomedicine Nanotechnology, Biol. Med.* **6**, 170–178 (2010).
87. Elsawy, M. A., Kim, K.-H., Park, J.-W. & Deep, A. Hydrolytic degradation of polylactic acid (PLA) and its composites. *Renew. Sustain. Energy Rev.* **79**, 1346–1352 (2017).
88. PANYAM, J., ZHOU, W.-Z., PRABHA, S., SAHOO, S. K. & LABHASETWAR, V. Rapid endo-lysosomal escape of poly(DL-lactide-co-glycolide) nanoparticles: implications for drug and gene delivery. *FASEB J.* **16**, 1217–1226 (2002).
89. Uskokovic, D. & Stevanovic, M. Poly(lactide-co-glycolide)-based Micro and Nanoparticles for the Controlled Drug Delivery of Vitamins. *Curr. Nanosci.* **5**, 1–14 (2009).
90. Peppas, N. A. & Narasimhan, B. Mathematical models in drug delivery: How modeling has shaped the way we design new drug delivery systems. *J. Control. Release* **190**, 75–81 (2014).
91. Makadia, H. K. & Siegel, S. J. Poly Lactic-co-Glycolic Acid (PLGA) as Biodegradable Controlled Drug Delivery Carrier. *Polymers (Basel).* **3**, 1377–1397 (2011).
92. Mohammad, A. K. & Reineke, J. J. Quantitative Detection of PLGA Nanoparticle Degradation in Tissues following Intravenous Administration. *Mol. Pharm.* **10**, 2183–2189 (2013).
93. Hickey, J. W., Santos, J. L., Williford, J.-M. & Mao, H.-Q. Control of polymeric nanoparticle size to improve therapeutic delivery. *J. Control. Release* **219**, 536–547 (2015).
94. Silva, A. L. *et al.* Functional Moieties for Intracellular Traffic of Nanomaterials. in *Biomedical Applications of Functionalized Nanomaterials: Concepts, Development and Clinical Translation* 399–448 (Elsevier, 2018). doi:10.1016/B978-0-323-50878-0.00014-8
95. He, L.-Z. *et al.* Antigenic Targeting of the Human Mannose Receptor Induces Tumor Immunity. *J. Immunol.* **178**, 6259–6267 (2007).
96. Foroozandeh, P. & Aziz, A. A. Insight into Cellular Uptake and Intracellular Trafficking of Nanoparticles. *Nanoscale Res. Lett.* **13**, 339 (2018).
97. Yingchoncharoen, P., Kalinowski, D. S. & Richardson, D. R. Lipid-Based Drug Delivery Systems in Cancer Therapy: What Is Available and What Is Yet to Come. *Pharmacol. Rev.* **68**, 701–787 (2016).
98. Yue, Z.-G. *et al.* Surface Charge Affects Cellular Uptake and Intracellular Trafficking of Chitosan-Based Nanoparticles. *Biomacromolecules* **12**, 2440–2446 (2011).
99. Benjaminsen, R. V., Mattebjerg, M. A., Henriksen, J. R., Moghimi, S. M. & Andresen, T. L. The Possible "Proton Sponge " Effect of Polyethylenimine (PEI) Does Not Include Change in Lysosomal pH. *Mol. Ther.* **21**, 149–157 (2013).
100. Bilensoy, E. Cationic nanoparticles for cancer therapy. *Expert Opin. Drug Deliv.* **7**, 795–809 (2010).
101. Zhang, L., Wang, W. & Wang, S. Effect of vaccine administration modality on immunogenicity and efficacy. *Expert Rev. Vaccines* **14**, 1509–1523 (2015).
102. Jiang, H., Wang, Q. & Sun, X. Lymph node targeting strategies to improve vaccination efficacy. *J. Control. Release* **267**, 47–56 (2017).
103. Manolova, V. *et al.* Nanoparticles target distinct dendritic cell populations according to their size. *Eur. J. Immunol.* **38**, 1404–1413 (2008).

104. Watts, P. J. & Smith, A. Re-formulating drugs and vaccines for intranasal delivery: maximum benefits for minimum risks? *Drug Discov. Today* **16**, 4–7 (2011).
105. Ansary, R. H., Awang, M. B. & Rahman, M. M. Biodegradable Poly(D,L-lactic-co-glycolic acid)-Based Micro/Nanoparticles for Sustained Release of Protein Drugs - A Review. *Trop. J. Pharm. Res.* **13**, 1179 (2014).
106. Nagavarma, B. V. N., Yadav, H. K. S., Ayaz, A., Vasudha, L. S. & Shivakumar, H. G. Different techniques for preparation of polymeric nanoparticles- A review. *Asian J. Pharm. Clin. Res.* **5**, 16–23 (2012).
107. Zupančič, E. *et al.* Rational design of nanoparticles towards targeting antigen-presenting cells and improved T cell priming. *J. Control. Release* **258**, (2017).
108. Iqbal, M., Zafar, N., Fessi, H. & Elaissari, A. Double emulsion solvent evaporation techniques used for drug encapsulation. *Int. J. Pharm.* **496**, 173–190 (2015).
109. Ding, S., Serra, C. A., Vandamme, T. F., Yu, W. & Anton, N. Double emulsions prepared by two–step emulsification: History, state-of-the-art and perspective. *J. Control. Release* **295**, 31–49 (2019).
110. Martinez, N. Y., Andrade, P. F., Durán, N. & Cavalitto, S. Development of double emulsion nanoparticles for the encapsulation of bovine serum albumin. *Colloids Surfaces B Biointerfaces* **158**, 190–196 (2017).
111. Conniot, J. Multicomponent Particulates for Immune Modulation, 2018
112. Turk, S., C., C., Badilli, Z. & Ullya, U. Preparation of polymeric nanoparticles using different stabilizing agents. *Ankara Univ. Eczac. Fak. Derg.* **38**, 257–268 (2009).
113. Strehl, C. *et al.* Effects of PVA coated nanoparticles on human immune cells. *Int. J. Nanomedicine* **10**, 3429 (2015).
114. Turk, C. T. S., Oz, U. C., Serim, T. M. & Hascicek, C. Formulation and Optimization of Nonionic Surfactants Emulsified Nimesulide-Loaded PLGA-Based Nanoparticles by Design of Experiments. *AAPS PharmSciTech* **15**, 161–176 (2014).
115. Zupančič, E., Silva, J., Videira, M. A., Moreira, J. N. & Florindo, H. F. Development of a Novel Nanoparticle-based Therapeutic Vaccine for Breast Cancer Immunotherapy. *Procedia Vaccinol.* **8**, 62–67 (2014).
116. Mora-Huertas, C. E., Fessi, H. & Elaissari, A. Polymer-based nanocapsules for drug delivery. *Int. J. Pharm.* **385**, 113–142 (2010).
117. Kennedy, P. J. *et al.* Impact of surfactants on the target recognition of Fab-conjugated PLGA nanoparticles. *Eur. J. Pharm. Biopharm.* **127**, 366–370 (2018).
118. Guo, Y., Luo, J., Tan, S., Otieno, B. O. & Zhang, Z. The applications of Vitamin E TPGS in drug delivery. *Eur. J. Pharm. Sci.* **49**, 175–186 (2013).
119. Yang, C., Wu, T., Qi, Y. & Zhang, Z. Recent Advances in the Application of Vitamin E TPGS for Drug Delivery. *Theranostics* **8**, 464–485 (2018).
120. Sahin, A. *et al.* Using PVA and TPGS as combined emulsifier in nanoprecipitation method improves characteristics and anticancer activity of ibuprofen loaded PLGA nanoparticles. *Pharmazie* **72**, 525–528 (2017).
121. Lakkadwala, S., Nguyen, S., Nesamony, J., Narang, A. S. & Boddu, S. H. Smart Polymers in Drug Delivery. in *Excipient Applications in Formulation Design and Drug Delivery* **77**, 169–199 (Springer International Publishing, 2015).
122. Sobczyński, J., Kristensen, S. & Berg, K. The influence of Pluronics nanovehicles on dark cytotoxicity, photocytotoxicity and localization of four model photosensitizers in cancer cells. *Photochem. Photobiol. Sci.* **13**, 8–22 (2014).
123. Coeshott, C. M. *et al.* Pluronic® F127-based systemic vaccine delivery systems. *Vaccine* **22**, 2396–2405 (2004).
124. Zhang, M., Yang, B., Liu, W. & Li, S. Influence of hydroxypropyl methylcellulose, methylcellulose, gelatin, poloxamer 407 and poloxamer 188 on the formation and

stability of soybean oil-in-water emulsions. *Asian J. Pharm. Sci.* **12**, 521–531 (2017).
125. Santander-Ortega, M. J., Jódar-Reyes, A. B., Csaba, N., Bastos-González, D. & Ortega-Vinuesa, J. L. Colloidal stability of Pluronic F68-coated PLGA nanoparticles: A variety of stabilisation mechanisms. *J. Colloid Interface Sci.* **302**, 522–529 (2006).
126. Freichels, H., Pourcelle, V., Auzély-Velty, R., Marchand-Brynaert, J. & Jérôme, C. Synthesis of poly(lactide-co-glycolide-co-ε-caprolactone)-graft- mannosylated poly(ethylene oxide) copolymers by combination of 'clip' and 'click' chemistries. *Biomacromolecules* **13**, 760–768 (2012).
127. Conniot, J. *et al.* Immunization with mannosylated nanovaccines and inhibition of the immune-suppressing microenvironment sensitizes melanoma to immune checkpoint modulators. *Nat. Nanotechnol.* (2019). doi:10.1038/s41565-019-0512-0
128. Aderibigbe, B. In Situ-Based Gels for Nose to Brain Delivery for the Treatment of Neurological Diseases. *Pharmaceutics* **10**, 40 (2018).
129. Guerrini, L., Alvarez-Puebla, R. A. & Pazos-Perez, N. Surface modifications of nanoparticles for stability in biological fluids. *Materials* **11**, 1154 (2018).
130. De, S. & Robinson, D. H. Particle size and temperature effect on the physical stability of PLGA nanospheres and microspheres containing Bodipy. *AAPS PharmSciTech* **5**, 18–24 (2004).
131. Mohammadi-Samani, S. & Taghipour, B. PLGA micro and nanoparticles in delivery of peptides and proteins; problems and approaches. *Pharm. Dev. Technol.* **20**, 385–393 (2015).
132. Bahuguna, A., Khan, I., Bajpai, V. K. & Kang, S. C. MTT assay to evaluate the cytotoxic potential of a drug. *Bangladesh J. Pharmacol.* **12**, 8 (2017).
133. Riccardi, C. & Nicoletti, I. Analysis of apoptosis by propidium iodide staining and flow cytometry. *Nat. Protoc.* **1**, 1458–1461 (2006).
134. Chen, S., Li, L., Zhao, C. & Zheng, J. Surface hydration: Principles and applications toward low-fouling/nonfouling biomaterials. *Polymer (Guildf).* **51**, 5283–5293 (2010).
135. Sharma, N., Madan, P. & Lin, S. Effect of process and formulation variables on the preparation of parenteral paclitaxel-loaded biodegradable polymeric nanoparticles: A co-surfactant study. *Asian J. Pharm. Sci.* **11**, 404–416 (2016).
136. Koppolu, B. & Zaharoff, D. A. The effect of antigen encapsulation in chitosan particles on uptake, activation and presentation by antigen presenting cells. *Biomaterials* **34**, 2359–2369 (2013).
137. Carrillo-Conde, B. *et al.* Mannose-Functionalized "Pathogen-like" Polyanhydride Nanoparticles Target C-Type Lectin Receptors on Dendritic Cells. *Mol. Pharm.* **8**, 1877–1886 (2011).
138. Bhatia, S., Edidin, M., Almo, S. C. & Nathenson, S. G. B7-1 and B7-2: Similar costimulatory ligands with different biochemical, oligomeric and signaling properties. *Immunol. Lett.* **104**, 70–75 (2006).
139. Ma, D. Y. & Clark, E. A. The role of CD40 and CD154/CD40L in dendritic cells. *Semin. Immunol.* **21**, 265–272 (2009).